AWARD NUMBER: W81XWH-21-1-0061

TITLE: Identification of the Precise Developmental Window and Tissue Bed for the Somatic Mutation Causing Sturge Weber Syndrome

PRINCIPAL INVESTIGATOR: Douglas A Marchuk, Ph.D.

CONTRACTING ORGANIZATION: Duke University

REPORT DATE: MAY 2023

TYPE OF REPORT: Final

PREPARED FOR: U.S. Army Medical Research and Development Command
Fort Detrick, Maryland 21702-5012

REPORT DOCUMENTATION PAGE

Form Approved
OMB No. 0704-0188

1. REPORT DATE	2. REPORT TYPE.	3. DATES COVERED
MAY 2023	FINAL	15JAN2021 - 14JAN2023

4. TITLE AND SUBTITLE

Identification of the Precise Developmental Window and Tissue Bed for the Somatic Mutation Causing Sturge Weber Syndrome

5a. CONTRACT NUMBER

W81XWH-21-1-0061

5b. GRANT NUMBER

W81XWH-21-1-0061

5c. PROGRAM ELEMENT NUMBER

6. AUTHOR(S)

Douglas A. Marchuk, PhD

E-Mail: douglas.marchuk@duke.edu

5d. PROJECT NUMBER

5e. TASK NUMBER

5f. WORK UNIT NUMBER

7. PERFORMING ORGANIZATION NAME(S) AND ADDRESS(ES)

Duke University
Durham, NC 27710

8. PERFORMING ORGANIZATION REPORT NUMBER

9. SPONSORING / MONITORING AGENCY NAME(S) AND ADDRESS(ES)

U.S. Army Medical Research and Development Command
Fort Detrick, Maryland 21702-5012

10. SPONSOR/MONITOR'S ACRONYM(S)

11. SPONSOR/MONITOR'S REPORT NUMBER(S)

12. DISTRIBUTION / AVAILABILITY STATEMENT

Approved for Public Release; Distribution Unlimited

13. SUPPLEMENTARY NOTES

14. ABSTRACT. Sturge Weber syndrome (SWS) is a sporadic, congenital, neuro-cutaneous disorder characterized by a capillary vascular malformation. The vascular malformation affects the skin in the distribution of the ophthalmic branch of the trigeminal nerve, and abnormal capillary venous vessels in the leptomeninges of the brain and choroid, leading to glaucoma, seizures, stroke, and intellectual disability. In 2013, a somatic mutation (c.548G→A, p.R183Q) in GNAQ (encoding Gαq) was identified in affected tissue from Sturge Weber Syndrome. This Gαq signaling pathway has been extensively studied in other biological and disease (cancer) contexts, and thus, potential drugs are already available. In addition, novel therapies that target this pathway are currently under development in biotech/pharma drug pipelines. The discovery of the cause of Sturge Weber Syndrome as this specific somatic activating mutation brought great hope of a scientifically-based treatment.

In order to translate fundamental somatic mutation discoveries to potential drugs that can be used in clinical practice, is it critical that animal models are developed for these vascular malformations. However, unlike Mendelian diseases, where the orthologous constitutional (germline) mutation can be easily generated in mice, it has proven quite difficult to develop mouse models that will spontaneously develop a specific, somatic mutation. The mutation cannot be passed through the germline, but must be induced during the development and/or growth of the animal. This difficulty is compounded by the requirement that the somatic mutation must be induced only in the correct tissue bed or organ, and in some cases, precisely within the correct window of time, possibly in a progenitor cell that exists only during that developmental window. It is especially difficult to generate an animal model if the somatic mutation must be induced *during development in utero*. This is precisely the pathobiological context for Sturge Weber Syndrome. It is perhaps not surprising that no animal model has been developed for Sturge Weber Syndrome, leading to a lack of studies testing potential therapies.

Our proposal addresses this most difficult clinical context. We propose that two critical questions must be addressed in order to generate a mouse model of SWS. The first critical question is which cell type and tissue bed acquires the GNAQ somatic mutation? The second critical question is when during development must the somatic mutation occur? We hypothesize that the lack of a mouse model for SWS is due to attempting to create the animal model in a single step - essentially requiring knowledge of the correct answer to both questions to be determined *at once*. By contrast, my lab has now developed the murine genetic tools (genetically-engineered mice) that enable us to systematically tackle the two gaps in knowledge by separating the two questions into parallel studies. Our approach utilizes a reporter mouse strain to address the developmental timing window knowledge gap and testing a battery of Cre-drivers to address the tissue bed/progenitor cell gap. Since the goal each aim is to address a specific question about the VM pathobiology but not to generate the final animal model, the aims can run in parallel, even with one approach outpacing the other. Once both questions are answered, we can combine the two approaches to create a mouse model.

While our study will focus on one particular vascular malformation, our approach can be used for other vascular malformations caused by a somatic mutation. Most importantly, what we learn about Sturge Weber Syndrome pathogenesis using our model will inform us about the pathogenesis of a broad spectrum of vascular malformations. Equally importantly, our approach will serve as a roadmap to develop mouse models and study the pathogenesis of other congenital phenotypes that occur as a result of somatic mutations occurring in utero.

15. SUBJECT TERMS

NONE LISTED

16. SECURITY CLASSIFICATION OF:			**17. LIMITATION OF ABSTRACT**	**18. NUMBER OF PAGES**	**19a. NAME OF RESPONSIBLE PERSON**
					USAMRDC
a. REPORT	**b. ABSTRACT**	**c. THIS PAGE**	UU	48	**19b. TELEPHONE NUMBER** *(include area code)*
U	U	U			

TABLE OF CONTENTS

1. Introduction

Sturge Weber syndrome (SWS) is a sporadic, congenital, neuro-cutaneous disorder characterized by a capillary vascular malformation. The vascular malformation affects the skin in the distribution of the ophthalmic branch of the trigeminal nerve, and abnormal capillary venous vessels in the leptomeninges of the brain and choroid, leading to glaucoma, seizures, stroke, and intellectual disability. In 2013, a somatic mutation (c.548G→A, p.R183Q) in GNAQ (encoding Gαq) was identified in affected tissue from Sturge Weber Syndrome. To date, no genetically faithful animal model has been developed for Sturge Weber Syndrome, leading to a lack of studies testing potential therapies. Our proposal addresses this gap by addressing two critical unsolved questions. The first critical question is which cell type and tissue bed acquires the GNAQ somatic mutation? The second critical question is when during development must the somatic mutation occur? My lab has now developed the murine genetic tools (genetically-engineered mice) that enable us to systematically tackle the two gaps in knowledge by separating the two questions into parallel studies. Our approach utilizes a reporter mouse strain to address the developmental timing window knowledge gap and testing a battery of Cre-drivers to address the tissue bed/progenitor cell gap. Since the goal each aim is to address a specific question about the VM pathobiology, the aims can run in parallel, even with one approach outpacing the other. Once both questions are answered, we can combine the two approaches to create a mouse model.

2. Keywords

Vascular malformation, mouse models of disease, somatic mutation, G protein, development

3. Accomplishments

Major Goals of Project.

Specific Aim 1: To identify a gene promoter and the (fetal) cell type acquires the somatic GNAQ mutation.	**Months**	**Site**
Major Task 1: Identify the proper promoter that will form VMs in the vascular beds associated with the SWS phenotype.	1-18	Duke Univ.
Subtask 1: Determination of correlation of recombination efficiency and mutant trans gene expression Mouse lines used: Our novel GNAQ mutant line crossed line to the mT/mG reporter line (ROSAmT/mG)	1-12	February 2022
Subtask 2: Examination of neonates or embyros for VMs in skin, brain leptomeninges, and other tissues. Mouse lines used: with various transgenic Cre-drivers including E2A-Cre, Slco1c1(BAC)-CreERT2, PDGFb-iCreERT2, and others as needed. Recombination efficiency determined by crossing GNAQ mutant	1-18	August 2022
Milestone(s) Achieved: Identification of one or more Cre-drivers that recapitulate VMs in disease relevant vascular beds.		achieved
Specific Aim 2: To determine the developmental time window that recapitulates expression in the organs and tissue beds affected in human SWS patients.		
Major Task 1: Identify developmental timing of GNAQ Mutation		Duke Univ.
Subtask 1: Identify optimal dose of tamoxifen injection for mosaic beta-galactosidase staining. Mouse lines used: ROSAβgeo26 (ROSA26) and PDGFb-iCreERT2 and other Cre-drivers	1-6	July 2021
Subtask 2: Identify optimal time of tamoxifen injection for mosaic beta-galactosidase staining. Mouse lines used: ROSAβgeo26 (ROSA26) and PDGFb-iCreERT2 and other Cre-drivers.	1-18	September 2022
Milestone(s) Achieved: Identification of the developmental window (gestational age) and technical details of tamoxifen dose that exhibits mosaic lacZ reporter expression in the vascular beds associated with SWS the phenotype.		achieved
Major Task 3: Generation of SWS mouse models exhibiting clinically-relevant phenotypes	12-24	Duke Univ.
Combination of dose and timing information determined from Aim 1 and different Cre-drivers from Aim 2 to generate one or more models that exhibit VMs in a disease relevant manner.		January 2023

Milestone(s) Achieved: Mouse models of SWS for future mechanistic and therapeutic studies		Not fully achieved since to date, model animals do not survive to birth

What was accomplished under these goals?

Please note that these same figures and tables - and more - are part of a revised, "provisionally accepted" manuscript that is appended to this application. This revision was submitted to the journal "Genetics" (the journal of the Genetics Society of America, GSA) on March 21 for final review.

We created a "conditional", floxed allele of the mouse Gnaq gene that expresses the wild-type version of the transcript, but upon Cre recombination, would express the mouse equivalent of the p.R183Q mutation. Cre is delivered by a transgene that is crossed into the conditional mouse line. Thus, our goal was to first show that this conditional allele performed as expected. The figure below shows the final floxed allele construct (and how it was generated) construct and that upon Cre recombination, the mutant version of the transcript.

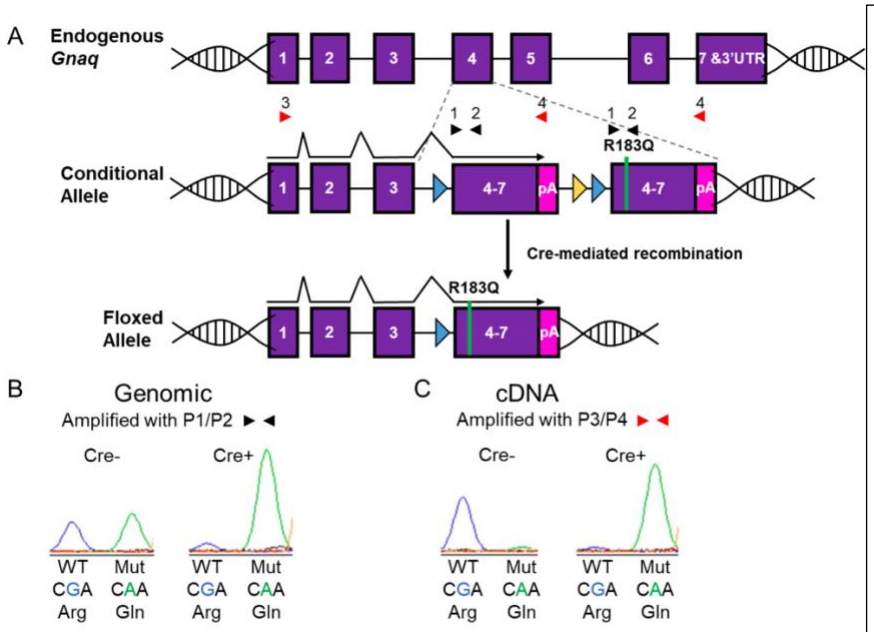

Fig 1. A. The conditional allele was recombined into the endogenous mouse Gnaq locus so that it remains under its normal regulatory control of expression. When the floxed allele undergoes further recombination by Cre recombinase (delivered by crossing this line to a transgenic line expressing Cre recombinase), the mutant version of exons 4-7 of the gene replace the wild-type version of the gene. Experimental Validation. B. At the genomic DNA level, control animals show both versions of exons 4-7 of the construct, but once Cre is expressed, the mutant version of Gnaq (identified by the green peak) has now replaced the wild-type version. C. At the RNA level, without Cre recombination, only the wild-type Gnaq transcript is expressed, but upon Cre recombination (here delivered by a beta-actin Cre mouse line, the mutant transcript is now expressed.

Having validated the expression of wild-type and mutant Gnaq transcript from the conditional allele *in vivo*, we were able to identify two different Cre-drivers that generated a vascular malformation phenotype. We first crossed our *Gnaq*RQ strain to a global Cre transgene, E2a-Cre, under the control of the adenovirus E2a promoter. E2a-Cre mediated recombination occurs early in the mouse embryo in a broad range of tissues, but

recombination efficiency varies widely across tissues and animals. We therefore examined *Gnaq* transcript levels in the *Gnaq*RQ$^{fl/wt}$;E2a-Cre+ embryos and found that levels of mutant transcript ranged between 43% to 100% while the *Gnaq*RQ$^{fl/wt}$ embryos had 0% mutant transcript detectable (data available in the appended manuscript). This range of mutant allele expression is expected due to the mosaic expression of the E2a Cre. In this cross, *Gnaq*RQ$^{fl/wt}$ x E2a-Cre+/+, we did observe survival to birth of some *Gnaq*RQ$^{fl/wt}$;E2a-Cre+ mice, but survival of this genotype was statistically below expected values. Genotyping of the offspring revealed that of 93 live-born mice, 15 were *Gnaq*RQ$^{fl/wt}$;E2a-Cre+ vs 78 *Gnaq*RQ$^{wt/wt}$;E2a-Cre+, representing a significant reduction from the expected 50% ratio for the cross (p*** <0.001; chi-square test).

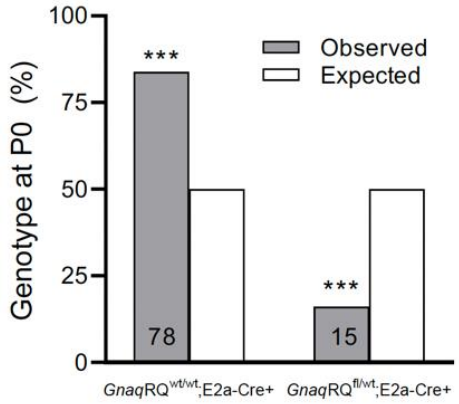

Figure 2. Reduced survival (live-born pups) of mice with the genotype containing both the Gnaq conditional allele and E2a-Cre transgenic recombinase. In this cross between an animal homozygous for the Cre transgene and heterozygous for the Gna1 conditional allele, we expect a 50:50 ratio of the two possible genotypes. Survival is well below expected values and highly significant.

Due to the decreased number of live-born animals of the *Gnaq*RQ$^{fl/wt}$;E2a-Cre+ genotype, we sought to determine if there were any embryonic phenotypes associated with the observed loss of these mice during development. Therefore, we dissected embryos at e13.5-14.5 for gross morphological evaluation and genotyping. At this stage of development, we found normal, Mendelian ratios for all the expected genotypes (differences not significant by Chi-square test). However, in *Gnaq*RQ$^{fl/wt}$;E2a-Cre+ embryos, we observed prominent edema and some dilated small vessels in 50% (5 out of 10) and 20% (2 of 10) of the animals, respectively. These findings indicated that mosaic expression of the mutant allele results in a severe embryonic phenotype in a significant number of *Gnaq*RQ$^{fl/wt}$;E2a-Cre+ mice that can eventually result in premature death.

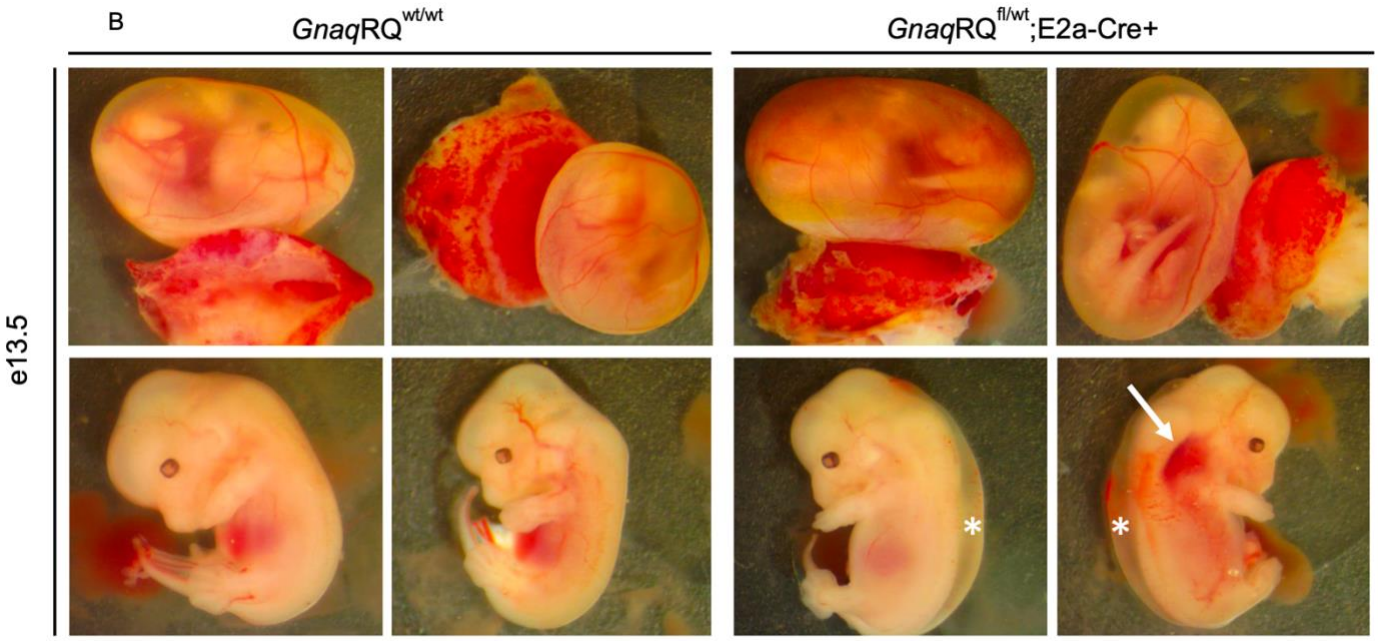

Figure 3. Edema and vascular malformations in the *Gnaq*RQ$^{fl/wt}$;E2a-Cre+ embryos. Control embyros (e13.5) without the conditional allele do not exhibit edema or evidence of vascular dilation, but the embryos with the conditional allele and the E2a Cre transgene show both edema (*) and vascular dilation (arrow). Thus, expression of the mutant allele of the Gnaq transcript is causing phenotypes consistent with what would be expected in a SWS human embryo. We assume these animals generally do not survive to birth, and thus, the number of live born pups is severely reduced. It entirely likely that the same occurs in SWS with humans and only those with a very low level of mosacism survive to birth.

Global expression of p.R183Q GNAQ is incompatible with survival

Our findings in the *Gnaq*RQ$^{fl/wt}$;E2a-Cre+ mice suggest that mosaic expression of the *Gnaq* mutant allele (p.R183Q) during development causes different degrees of pathology, the extent of which are likely due to the tissue location and the expression level of the mutant allele. Therefore, we next investigated the effect of global p.R183Q expression to determine if early global embryonic expression of the p.R183Q GNAQ mutation is compatible with survival. For this experiment, we crossed our *Gnaq*RQ conditional mutant strain with a transgenic line expressing a global (ubiquitous) β-actin Cre driver where the recombination occurs in the entire soma as early as the blastocyst stage.

Genotyping of mice at P0 in the cross between the β-actin Cre driver and our *Gnaq* inducible construct showed that no live-born mice contained both the Cre driver and the *Gnaq* conditional allele (Table 1; below) indicating that the p.R183Q GNAQ mutation causes embryonic lethality when globally expressed during the earliest stages of development.

Number of mice/ genotype					
Age	Total number	*Gnaq*RQ$^{wt/wt}$	*Gnaq*RQ$^{wt/wt}$; β-actin-Cre^{+}	*Gnaq*RQ$^{fl/wt}$	*Gnaq*RQ$^{fl/wt}$; β-actin-Cre^{+}
e14.5	70	15	22	19	14
P0	77	24	28	25	0

Table 1. In a cross between a mouse heterozygous for the GnaqRQ conditional allele and the β-actin Cre driver, where all four genotype classes (WT, heterozygous for each construct, and double hets – the embryos that would express the mutant Gnaq transcript - are expected at equal ratios. The frist three are found in approximately equal numbers as expected, but NO live born pups are seen for the double heterozygous class. Thus, expression of the mutant Gnaq with this "globally-expressed" Cre driver is incompatible with survival to birth.

To determine if and when the embryos expressing the mutant allele were present and if they displayed any phenotype, we examined mouse embryos at different stages of development. In initial observations of e11.5 and e14.5 embryos from crosses that would only yield β-actin-Cre positive embryos, we saw equal numbers of *Gnaq*RQ$^{wt/wt}$; Cre+ and *Gnaq*RQ$^{fl/wt}$;Cre+ embryos (data not shown). At e11.5, none of the embryos appeared different than littermate controls, but at e14.5, *Gnaq*RQ$^{fl/wt}$;Cre+ embryos did show an overt vascular phenotype.

Embryonic death in GnaqRQ$^{fl/wt}$;β-actin-Cre+ animals is associated with hemorrhage and vasodilation

Gross examination of *Gnaq*RQ$^{fl/wt}$;β-actin-Cre+ embryos demonstrated a variable phenotype. Although a small fraction of the *Gnaq*RQ$^{fl/wt}$;β-actin-Cre+ embryos appeared similar to their control littermates, a much higher percentage of *Gnaq*RQ$^{fl/wt}$;β-actin-Cre+ embryos demonstrated subcutaneous hemorrhage, edema, or were pale in color compared to controls. Genotype blinded examination of e14.5 embryos of all 4 possible genotypes showed hemorrhage in 86% of the *Gnaq*RQ$^{fl/wt}$;β-actin-Cre+ animals, which was often associated with subcutaneous edema (71%). By contrast, control littermates of all other genotypes did not exhibit any strong pathologies (Figure 4A). Mild hemorrhage and edema was reported only in one *Gnaq*RQ$^{wt/wt}$ embryo and in one *Gnaq*RQ$^{wt/wt}$;β-actin-Cre+ embryo, confirming that the severe phenotypes observed in *Gnaq*RQ$^{fl/wt}$;β-actin-Cre+ mice were associated with the expression of the mutant R183Q allele during development.

Genotype (e14.5)	Total number of embryos	Embryos with vascular anomaly	Embryos with edema
*Gnaq*RQ$^{wt/wt}$	15	1 (7%)	0
*Gnaq*RQ$^{wt/wt}$;β-actin-Cre+	22	0	1 (4%)
*Gnaq*RQ$^{fl/wt}$	19	0	0
*Gnaq*RQ$^{fl/wt}$;β-actin-Cre+	14	12 (86%)	10 (71%)

Table 2. The majority of e14.5 GnaqRQ embryos under the β-actin Cre driver show vascular anomalies and edema. In a cross between GnaqRQ conditional animals and β-actin Cre animals resulting in all 4 possible genotypes, two independent, genotype-binded investigators visualized the embryos under 10X magnification and scored for edema and/or a visible vascular anomaly. While a single control genotype animal for two genotypes showed visible edema or a vascular anomaly, the great majority of GnaqRQ conditional allele embryos that also have the β-actin Cre driver show both vascular anomalies and/or edema. Thus, embryos expressing the mutant version of Gnaq transcript exhibit SWS-associated embryonic phenotypes.

As most of these e14.5 embryos exhibited vascular abnormalities during gross examination, we performed histological assessment. Sagittal sections of the whole embryo revealed areas of extravasation in the subcutaneous region in *Gnaq*RQ$^{fl/wt}$;β-actin-Cre+ embryos, indicating severe alteration of blood vessel formation and circulation. Moreover, PECAM-1 immunostaining confirmed the presence of dilated blood vessels filled with red blood cells at sites of apparent hemorrhage in *Gnaq*RQ$^{fl/wt}$;β-actin-Cre+ embryos, not seen in controls (Figure 4G and K). Instead, the blood vessels in *Gnaq*RQ$^{fl/wt}$ littermate controls were small, with only a few red blood cells visible in each vessel (Figure 4C, E, and I).

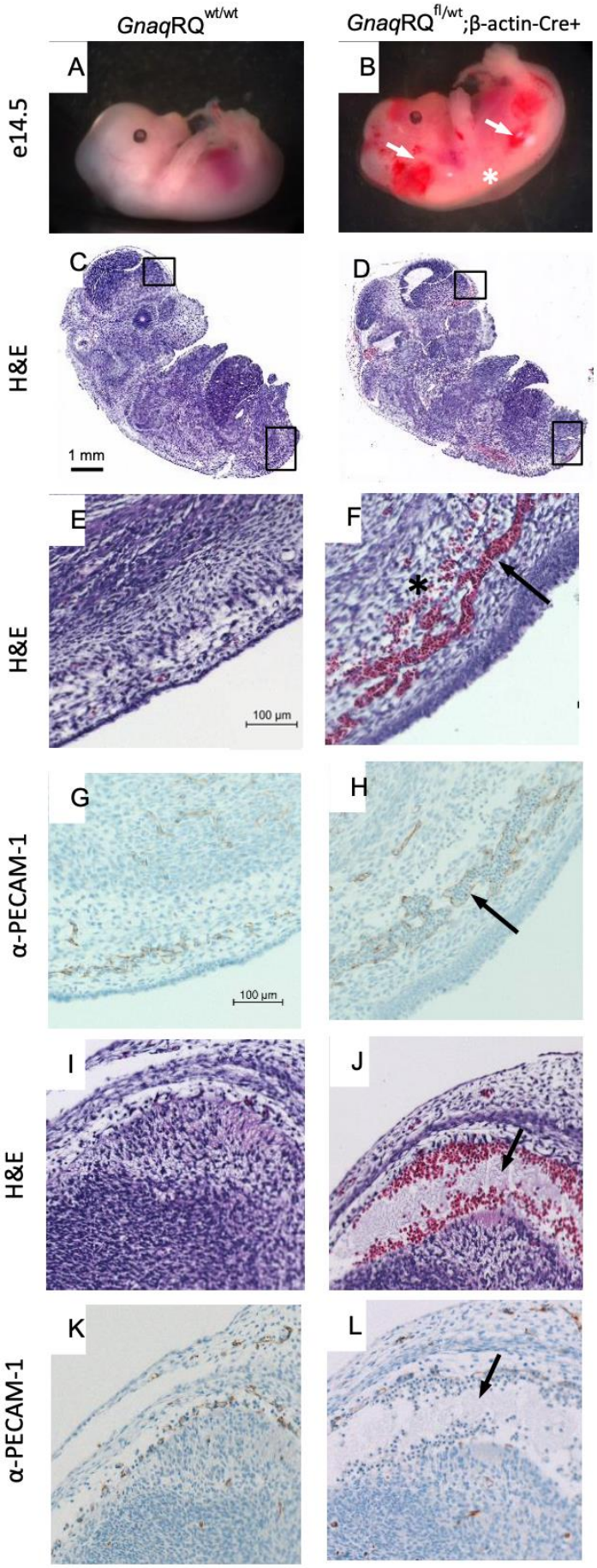

Figure 4. Histopathological analysis of tissue sections of e14.5 embryos from control and Gnaq conditional allele plus b-actin Cre driver transgene. Wild-type control embryos show no visible evidence of a vascular malformation (A) and histological analyses from two different regions,C even upon magnification (E, and I), show no evidence of vascular dilation or hemorrhage. By contrast, the Gnaq conditional allele with the b-actin Cre driver exhibits evidence of vascular dilation (B; arrows), in multiple regions (B and D) and edema (B; asterisk). This dilation and hemorrhage are even more evident with magnification (F and J). PECAM staining to reveal the endothelial layer of the blood vessels confirms that vessel dilation (arrows), a hallmark feature of SWS, not seen in control embryos (G and K) but is seen in the Gnaq condaitional allele animals with the Cre driver (H and L). There is also evidence of hemorrhage - blood cells outside the dilated vessel wall (asterisk in Panel F).

Brief Discussion of Significance. These data show that we have created a mouse model of SWS that exhibits disease-appropriate phenotypes, but to date, the phenotype is so severe that we haven't generated pups that survive to birth that still show this phenotype. We surmise that the mutant transcript needs to be expressed fewer cells in the developing embryo in order to survive to birth - fewer than we have yet to accomplish. Continued research will solve this issue. Nonetheless, our work has made a significant contribute to our understanding of SWS. SWS is never inherited – it is not passed from parent to offspring, and is only seen as a sporadic phenotype. Decades ago, Rudolf Happle (Freiburg, Germany) hypothesized that SWS would be caused by a mosaic, somatic mutation in a then, yet undetermined gene, that if mutated in every cell early in development, would be incompatible with life (survival to birth). He coined the term "paradominant inheritance" to mean a dominant mutation that can only occur in the mosaic state for survival to birth or beyond. We were part of the team that discovered the causative mutation for SWS in 2013, but to date, no one had tested Happle's hypothesis *in vivo*. Our data shown here confirms this decades-old hypothesis and provides the template for additional studies on the pathogenesis of SWS, as well as for further model development. Further details are provided in the appended manuscript, as well as a discussion of these data in light of the known etiology of SWS.

What opportunities for training and professional development has the project provided?

Although this project was not primary intended to provide training, Sarah Wetzel-Strong, PhD, mentored animal technician Mary Patrucco, in the analysis of tissue from embryos. Likewise, later on, Francesca Galeffi, MD, mentored animal technician Christian Benavides, in analysis of tissue from embryos. Thus our animal technicians were trained in laboratory techniques outside of mouse colony management and animal husbandry, which was their primary duty. Finally, a Duke undergraduate student, Jaye Bullock, performed molecular analyses of tissue samples from some of the embryos as part of her own undergraduate thesis project that was tangential to this DOD funded project. Her project was of her own design, using embryo tissue from our mouse model of SWS to address questions about gene expression effects of the mutation *in vivo*. Francesca Galeffi, MD, and others in the lab mentored her in molecular techniques and in scientific writing.

How were the results disseminated to communities of interest? Nothing to report.

What do you plan to do during the next reporting perios to accomplish these goals? As this is the final report, there is nothing further to report.

4. Impact

On the principal discipline. Our mouse model is the first model of SWS that faithfully replicates the origins of the somatic mutation *during development*, and the developmental nature of the vascular lesion. This is a significant milestone that will enable future mechanistic studies in vivo, and as novel therapies are suggested, a key animal model to be used in pre-clinical studies.

Other disciplines. Nothing to report.

Technology transfer. Nothing to report.

Impact on society beyond science and technology. Nothing to report.

5. Changes/Problems

No significant changes or problems

6. Products.

a. An original version of a manuscript describing this work was recently provisionally accepted for publication in *"Genetics",* for a special issue on "Genetic Models of Rare Diseases". A revised version of the manuscript was submitted on March 21, 2023, and is currently under final review. This revised version is included as an appendix in this report.

b. While a postdoctoral fellow in the lab, Sarah Wetzel-Strong PhD, presented an update on this work at a Sturge Weber Foundation International Research Foundation virtual meeting in 2021. In 2022, the PI, Douglas Marchuk, PhD presented a further update. These informal virtual meetings are held three times per year for a small network of scientists (8-12 attendees per session) working on SWS cellular and animal models of disease. The meetings are private and closed to the public and there are no recordings of these presentations.

c. The current SWS mouse model as presented in our publication would be considered another product of this study. The animal must be continuously generated by crosses between the Cre-driver line and the line with the conditional mutant allele which we generated. Upon publication, the conditional allele that we generated will be available for use by others.

7. Participants & Other Collaborating Organizations.

Name:	*Douglas Marchuk, Ph.D.*
Project Role:	*Project Leader*
Researcher Identifier (e.g. ORCID ID):	0000-0002-3110-6671
Nearest person month worked:	*2 months- thoughout entire duration of grant*
Contribution to Project:	*Scientific Leadership on all aspects of the project*
Funding Support:	*Part of Dr. Marchuk's salary comes from this DOD award, the rest comes from other NIH grants and other sources.*
Name:	*Sarah Wetzel-Strong, Ph.D.*
Project Role:	*Postdoctoral Fellow*
Researcher Identifier (e.g. ORCID ID):	0000-0001-5560-2330
Nearest person month worked:	*11 months - from January 15, 2021 through December 31, 2021*
Contribution to Project:	*Sarah was the primary postdoctoral fellow on this award at its intiation. This was her primary project until she left the lab at the end of December 2021 for another position. Sarah organized the animal breeding and analyzed all of the tissue at necropsy.*
Funding Support:	*Sarah was paid from this grant.*
Name:	*Francesca Galeffi, M.D.*
Project Role:	*Lab Analyst II*
Nearest person month worked:	*6 months; from January 1, 2022 to the end of the grant Jan 14, 2023.*
Contribution to Project:	*Francesca took over the project in January 2022, after Sarah Wetzel-Strong left the lab. Franceca had a major role on another project as well, so she worked on this project approximately half of her time. As Sarah did before her, Francesca organized the animal breeding and performed all of the analyses of tissue.*
Funding Support:	*Approximately half of Francesca's salary is paid from this DOD award, and her salary is also paid off another grant that funds her project on another topic.*
Researcher Identifier (e.g. ORCID ID):	*0009-0001-8973-8129*
Name:	*Mary Patrucco, B.S.*
Project Role:	*Laboratory Animal Technician*
Researcher Identifier (e.g. ORCID ID):	*NA*
Nearest person month worked:	*8 months - 30% effort from January 15, 2021 to April 30, 2022*
Contribution to Project:	*Mary was the primary animal technician on this project until she left for another position. Mary set up all the matings for the mouse crosses in the mouse colony and assisted Sarah Wetzel-Strong (and later, Francesca) in necropsy of mouse tissues.*

Funding Support:	*As with all of our animal technicians, Mary was only part time on this project as she has duties in the mouse colony for all of our projects. So she was paid off this DOD grant as well as others.*
Name:	*Christian Benavides. B.S.*
Project Role:	*Laboratory Animal Technician*
Nearest person month worked:	*6 months 30-40 % effort May 1 2022 to Jan 14, 2023 (end of grant)*
Contribution to Project:	*Chris took over primary animal duties on the SWS mouse project for Mary Patrucco after she left the lab at the end of April 2022. Chris then set up all the matings for the mouse crosses in the mouse colony and assisted Francesca in necropsy of mouse tissues.*
Funding Support:	*As with all of our animal technicians, Chris was only part time on this project as he has duties in the mouse colony for all of our projects. So he was paid off this DOD grant as well as others.*
Researcher Identifier (e.g. ORCID ID):	*NA*

No changes in active other support for key personnel during the duration of the grant funding (the only key personnel was Douglas Marchuk)

No other organizations involved as partners during the duration of this research project.

8. Special Reporting Requirements. Not applicable

9. Appendices.

The revised manuscript describing this work was submitted to "*Genetics*" on March 21, 2023.

Please see following pages.

Title: Developmental Expression of the Sturge-Weber Syndrome-associated Genetic Mutation in *Gnaq*: a Formal Test of Happle's Paradominant Inheritance Hypothesis.

Authors: Sarah E. Wetzel-Strong[1*], Francesca Galeffi[1*], Christian Benavides[1], Mary Patrucco[1], Jessica L. Bullock[1], Carol J. Gallione[1], Han Kyu Lee[1], Douglas A. Marchuk[1‡]

1. Department of Molecular Genetics and Microbiology, Duke University School of Medicine, Durham, NC 27710

*These two authors contributed equally.

‡ Corresponding author: Department of Molecular Genetics and Microbiology, Duke University School of Medicine, Durham, NC 27710, USA.

Keywords

G proteins, mouse models, rare disease

Abstract

Sturge-Weber Syndrome (SWS) is a sporadic (non-inherited) syndrome characterized by capillary vascular malformations in the facial skin, leptomeninges, or the choroid. A hallmark feature is the mosaic nature of the phenotype. SWS is caused by a somatic mosaic mutation in the GNAQ gene (p.R183Q), leading to activation of the G protein, Gαq. Decades ago, Rudolf Happle hypothesized SWS as an example of "paradominant inheritance", that is, a "lethal gene (mutation) surviving by mosaicism". He predicted that the "presence of the mutation in the zygote will lead to death of the embryo at an early stage of development". We have created a mouse model for SWS using gene

targeting to conditionally express the Gnaq p.R183Q mutation. We have employed two different Cre-drivers to examine the phenotypic effects of expression of this mutation at different levels and stages of development. As predicted by Happle, global, ubiquitous expression of this mutation in the blastocyst stage results in 100% embryonic death. The majority of these developing embryos show vascular defects consistent with the human vascular phenotype. By contrast, global but *mosaic* expression of the mutation enables a fraction of the embryos to survive, but those that survive to birth and beyond do not exhibit obvious vascular defects. These data validate Happle's paradominant inheritance hypothesis for SWS and suggest the requirement of a tight temporal and developmental window of mutation expression for the generation of the vascular phenotype. Furthermore, these engineered murine alleles provide the template for the development of a mouse model of SWS that acquires the somatic mutation during embryonic development, but permits the embryo to progress to live birth and beyond, so that postnatal phenotypes can also be investigated. These mice could then also be employed in pre-clinical studies of novel therapies.

Introduction

Sturge-Weber Syndrome (SWS) is a rare vascular malformation syndrome characterized by capillary vascular malformations that may be present in the facial skin, leptomeninges, or the choroid. A characteristic feature of SWS is the mosaic nature of the clinical phenotype. The facial capillary malformation is usually unilateral (Van Trigt et al. 2022), as are the leptomeningeal and choroidal vascular lesions. Together, these vascular malformations cause a severe decrease in the quality of life due to the stigma

associated with the facial vascular lesions, early vision loss due to glaucoma when choroidal lesions are present, as well as debilitating headaches, stroke-like ischemic events, and seizures due to the leptomeningeal lesions. To date, the phenotype appears sporadically, and importantly, there are no confirmed cases of inheritance from parent to child.

In 1987, Dr. Rudolf Happle proposed that SWS and other select mosaic phenotypes were due to somatic mutations in essential developmental genes, and that germline inheritance of these mutations would be lethal (Happle 1987); he coined the term 'paradominant inheritance' to describe the concept of a "lethal mutation surviving because of mosaicism". In 2013, the causative mutation of SWS was identified as the somatic, mosaic mutation c.548G>A, exchanging arginine 183 for glutamine (p.R183Q) in the gene *GNAQ*, encoding the G protein subunit alpha q protein (Shirley et al. 2013). Functional analysis has confirmed that this mutation activates the G protein, Gαq (GNAQ) (Shirley et al. 2013; Galeffi et al. 2022). However, the full consequences of the expression of this genetic mutation during embryonic development remain a point of conjecture because no study has addressed this critical question. Thus, the 'paradominant inheritance' hypothesis for SWS has yet to be experimentally validated.

Animal models are essential tools for biomedical research and are especially important for understanding disease processes in developmental disorders. Yet generating an animal model that faithfully recapitulates the SWS phenotype has been challenging. The somatic mutation is presumably acquired in a particular progenitor cell, likely of mesodermal origin (Uchiyama et al. 2016), but the precise identity of this progenitor cell

remains unknown, thereby hindering animal model development. Two mouse models of SWS have been published to date (Huang et al. 2022; Sasaki et al. 2022). Both rely on the implantation of mutant endothelial cells into the flank of athymic nude (*nu/nu*) mice, resulting in dilated vessels in the implanted xenograft. Although these models have provided important information about the consequences of these mutations within endothelial cells *in vivo*, they are unable to provide insight into the role of the p.R183Q GNAQ mutation during *in utero* development – a hallmark feature of the human syndrome. Thus, these models cannot test Happle's 'paradominant inheritance' hypothesis.

In this study, we developed a mouse model that allows for conditional expression of p.R183Q GNAQ from the endogenous mouse *Gnaq* locus. Through this approach, we tested whether early embryonic expression of this mutant is compatible with life and performed an initial examination of the phenotypes associated with expression of this mutation during embryonic development.

Methods and Materials

Mice

Mice with conditional expression of p.R183Q GNAQ were generated through gene targeting techniques by the Duke Transgenic and Knockout Mouse core. The targeting vector (shown in Figure S1) contained a cDNA segment encoding exons 4 through 7 of mouse *Gnaq* flanked by loxP sites, a neomycin resistance cassette flanked by FRT sites, and a cDNA segment encoding exons 4 through 7 of mouse *Gnaq* with the p.R183Q mutation. The 3'UTR and poly(A) site from Bovine growth hormone 1 (BGH1)

was ligated to the 3'-end of exon 7 substituting for the endogenous 3'UTR and poly(A) site to provide a way to distinguish transcripts arising from the conditional allele from transcripts arising from the untouched endogenous *Gnaq*. Because R183 is encoded in exon 4 of *Gnaq*, the homology arms were designed in the introns flanking exon 4 to direct replacement of the endogenous *Gnaq* exon 4 with the targeting construct. The resulting mice were named B6-*Gnaq*RQ^{tmR183Q}, referred to as *Gnaq*RQ. The conditional allele will be denoted as *Gnaq*RQ^{fl} and the endogenous wild-type (WT) allele as *Gnaq*RQ^{wt}. To remove the neo cassette, the *Gnaq*RQ mice were crossed with ACTB$^{FLPe/FLPe}$ mice (JAX stock #003800,(Rodriguez et al. 2000)). PCR genotyping confirmed removal of the neo cassette. Mice were backcrossed to C57Bl6/J mice for 5 generations to ensure a homogeneous genetic background for the experiments. *Gnaq*RQ$^{fl/wt}$ mice were first crossed to R26-CreERT2 (JAX stock #008463,(Ventura et al. 2007)) to determine the level of recombination on the conditional allele. 100ug of Tamoxifen (Sigma, T5648) was injected intra-gastrically to pups on P3 and the animals were euthanized and analyzed at various ages for the presence of mutant and WT transcript. In further experiments, *Gnaq*RQ$^{fl/wt}$ mice were crossed to either the β-actin-Cre (JAX stock # 019099, (Lewandoski et al. 1997)) or the E2a-Cre (JAX stock #003724, (Lakso et al. 1996)) lines to drive constitutive, global expression of p.R183Q GNAQ. Timed matings were performed and embryos were collected at different times during embryonic development or postnatal animals were assessed. Mice were genotyped for the presence of the conditional *Gnaq* allele, for R26-CreERT2, β-actin-Cre, and E2a-Cre by Transnetyx (Cordova, TN). All animal procedures were performed according to protocols approved by the Duke University IACUC.

RNA Isolation and cDNA Synthesis

Mouse tissue was flash frozen in liquid Nitrogen immediately after dissection and RNA was extracted using TRIzol after manual tissue disruption following the manufacturer's protocol (Invitrogen, 15596026). RNA concentrations were measured using a Nanodrop (Nanodrop One^{c}, Thermo Scientific, Waltham, MA, USA). Prior to cDNA synthesis, 1 µg of total RNA was DNase-treated (Invitrogen, 18068015). RNA was then used for cDNA synthesis with M-MLV primed by oligo(dT) following the manufacturer's protocol (Invitrogen, 28025013).

SNaPshot assay

Full-length *Gnaq* transcript was amplified from cDNA using Platinum Taq DNA Polymerase High Fidelity (Invitrogen, 113040110) with the following primers (Forward: 5′-CAGCTGCGCAGGGACAAG-3′; Reverse: 5′−AGGAAAGGACAGTGGGAGTG-3′) with the forward primer in exon 1 of *Gnaq* and the reverse primer in the 3' BGH1 UTR, according to the manufacturer's protocol. The PCR product was separated on a 1% agarose gel and gel-purified using GeneClean Turbo (MP Biomedical, 111102200CF). The SNaPshot single-base extension reaction was performed following the manufacturer's protocol using the following primers: (Top strand: 5′AAGACGTGCTTAGAGTTC-3′; Bottom strand: 5′CCCTGTAGTGGGGACT-3′). The sequencing data were analyzed on an ABI Prism 3130 Genetic Analyzer sequencer and peaks were determined using GeneMapper software. Percent recombination was calculated with the following formula: percent mutant allele frequency = ([mutant peak height] / [mutant + WT peak heights]) × 100%.

Quantitative Reverse Transcription PCR (qRT-PCR)

The mRNA levels of *Gnaq* (of both the endogenous and conditional alleles) and *Angpt2* in *Gnaq*RQ$^{fl/wt}$;β-actin-Cre+ embryos and *Gnaq*RQ$^{fl/wt}$ littermate controls were measured by quantitative PCR (qPCR) as previously described (Keum et al. 2013; Lee et al. 2022). Briefly, to determine transcript levels of *Gnaq* and *Angpt2* for each mouse embryo, mRNA was isolated from e14.5 mouse embryo tissue using TRIzol (Invitrogen, 15596026) and cDNA was synthesized as described above. Transcript levels of *Gnaq* and *Angpt2* from individual mouse embryos were quantitated using a dye-based qPCR method (iTaq Univeral SYBR Green Supermix, Bio-Rad, CA). All samples were run in triplicate, and an additional assay for endogenous *Gapdh* was performed to control for input cDNA template quantity. The primers used for qPCR reactions were as follows: *Gnaq,* Exon 3 (Forward): 5'-TACGACAGACGACGGGAATA-3', (endogenous and conditional alleles); 3' UTR (Reverse): 5'-CCCTCTTGTTTATCTTCAAC-3' (endogenous allele); BGH UTR (Reverse): 5'-GGCAAACAACAGATGGCTGG-3'(conditional allele); *Angpt2*: (Forward): 5'-ACAGCTGTGATGATAGAGATTGG-3', (Reverse): 5'-GTTGGAGAAGCTGCAGCTCG-3'; *Gapdh* (Forward): 5'-TCCCACTCTTCCACCTTCGA-3', (Reverse): 5'-AGTTGGGATAGGGCCTCTCTTG-3'.

Histology

For histological analysis, mouse embryos were removed at e14.5, fixed in 10% buffered formalin overnight, and then processed for paraffin embedding according to standard protocols. Sagittal sections of the entire embryo (6 μm thick) were stained with

hematoxylin and eosin (H&E). Alternating sections were incubated with anti-CD31 antibody (Abcam, Cambridge, CB2 0AX UK. Cat #ab28364) as a specific marker for vascular endothelial cells and then incubated with HRP-conjugated multimer antibody reagent. HRP-conjugated multimers, (Dics Omnimap anti-Rb HRP RUO, Roche, 1211 Vienna, Austria, Cat #760-4311) were used followed by DAB staining with the avidin-biotin complex peroxidase kit (Vectastain Elite, Newark, CA, 94560) and counterstained with Hematoxylin. Tissue processing for paraffin embedding and staining was performed by the Pathology and Histology Laboratory Research Core Facility at Duke. Images were obtained using a Zeiss microscope and Zen 3.5 Pro software. ImageJ software was used for measuring the subcutaneous vessel diameter.

Results

Generating a mouse model of conditional p.R183Q GNAQ expression

To determine the effect of the p.R183Q GNAQ mutation during development, we generated a conditional mouse model where we can modulate the expression of this mutation. As shown in Figure 1A, the engineered construct was integrated into the endogenous mouse *Gnaq* locus to place it under the gene's normal regulation and level of expression. The WT segment of the construct is flanked by loxP sites, which upon Cre recombination, is deleted from the locus. This Cre-mediated deletion of the WT genomic sequence from the conditional allele leaves the mutant construct intact and the resulting transcript will be spliced onto the first three exons of *Gnaq* from the endogenous gene (floxed allele). Thus, expression of WT or mutant transcript is regulated by Cre recombination. To determine the amount of genomic recombination, we amplified the region surrounding p.183. These primers amplify both the WT and

mutant DNA from the conditional allele but not from the endogenous *Gnaq* allele as the primers are located within exons 4 and 5, which are separated by a large intron in the endogenous locus (Figure 1A and B). A similar assay was designed so that when cDNA is used as the template, we could determine the ratio of WT to mutant transcript expression. Forward primers from the endogenous *Gnaq* exons 1 or 3 were paired with reverse primers specific to the novel 3'UTR found only on the conditional allele ensuring that these assays only monitor molecular events within the engineered construct - neither genomic DNA nor cDNA can amplify from the endogenous non-engineered allele (Figure 1A and C). We then designed a single base extension assay at the position of the mutation (SNaPshot) to distinguish the extent of recombination in the construct along with the level of WT vs mutant transcript. Using the genomic DNA assay, Figure 1B shows that the conditional expression system performs as expected; without Cre recombination, both WT and mutant are seen in roughly equal amounts, and with Cre recombination, the mutant transcript level is increased (Figure 1B). In cDNA from animals with Cre recombination, transcription is only seen from the mutant allele; there is no mutant transcript detectable in the Cre negative animals (Figure 1C).

Although we inserted the floxed engineered construct into the endogenous *Gnaq* locus, it is formally possible that this additional DNA might influence the gene's expression level. To determine whether the introduction of the construct into the endogenous *Gnaq* locus alters *Gnaq* transcript expression, we performed quantitative (q)RT-PCR for *Gnaq* endogenous and conditional alleles on mouse embryonic tissue from *Gnaq*RQ$^{fl/wt}$;β-actin-Cre+ and *Gnaq*RQ$^{fl/wt}$ littermate controls. We found that in both groups the levels of *Gnaq* conditional allele transcripts were significantly higher than the endogenous

allele (p*** = 0.0002 and p** = 0.007 conditional *vs* endogenous in *Gnaq*RQ$^{fl/wt}$ and *Gnaq*RQ$^{fl/wt}$;β-actin-Cre+ respectively, two tailed paired *t*-test) (Figure S2) with a greater increase in *Gnaq*RQ$^{fl/wt}$;β-actin-Cre+ (p*** <0.001 *Gnaq*RQ$^{fl/wt}$;β-actin-Cre+ *vs* *Gnaq*RQ$^{fl/wt}$, two tailed unpaired *t*-test) (Figure S2).

Another technical possibility is that due to the nature of the engineered conditional allele, the *Gnaq* mutant allele might undergo exon skipping. Using the GeneMapper software, we are able to detect allele frequencies of 1% and higher ((Shirley et al. 2013) and unpublished data) and to date, SNaPshot results from Cre negative animals using any of the Cre drivers do not show the mutant *Gnaq* allele at measurable levels. Additionally, we have been breeding the *Gnaq*RQ line for more than 10 generations and have not seen any overt phenotypic consequences: the mice are phenotypically normal, fertile, and there is no sex bias at birth or in longevity. Thus, if there is some nominal amount of mutant *Gnaq* expression, it is not having any demonstrable effect on the mice.

Effect of global but mosaic recombination of Gnaq mutant expression

We first crossed our *Gnaq*RQ strain to a global Cre transgene, E2a-Cre, under the control of the adenovirus E2a promoter. E2a-Cre mediated recombination occurs early in the mouse embryo in a broad range of tissues, but recombination efficiency varies widely across tissues and animals (Lakso et al. 1996). We reasoned that if Happle was correct, and the mutation would be lethal if acquired in all tissues, then mosaic recombination might permit survival of some of the developing embryos. In this cross, *Gnaq*RQ$^{fl/wt}$ x E2a-Cre+/+, we did observe survival to birth of some *Gnaq*RQ$^{fl/wt}$;E2a-

Cre+ mice, but survival of this genotype was statistically below expected values (Figure 2). Genotyping of the offspring revealed that of 93 live-born mice, 15 were *Gnaq*RQ$^{fl/wt}$;E2a-Cre+ vs 78 *Gnaq*RQ$^{wt/wt}$;E2a-Cre+, representing a significant reduction from the expected 50% ratio for the cross (p*** <0.001; chi-square test).

Some of the live-born pups were sacrificed at weaning (P21) for molecular analysis and phenotype assessment while others were allowed to age up to one year for observation of any overt phenotypes. In analysis of RNA from the liver, (the brains were used for other phenotypic analyses), the percentage of the mutant transcript ranged from 5.3% to 51.5% in *Gnaq*RQ$^{fl/wt}$;E2a-Cre+ animals of a range of ages, confirming *mosaic* Cre-mediated recombination and transcription of the mutant allele (Figure 3A). As expected with this Cre driver, recombination was incomplete and varied widely, leading to varied ratios of mutant to WT transcript in the survivors.

Because SWS patients can develop capillary malformations involving both the skin and/or brain leptomeninges, we performed a gross examination of the skin and the surface of the brains of *Gnaq*RQ$^{fl/wt}$;E2a-Cre+ and *Gnaq*RQ$^{fl/wt}$ littermates. During gross examination of newborn pups and later of 21-day old animals, we did not observe any obvious skin vascular phenotype or vascular abnormalities on the surface of the brains. However, in 11 out of 15 *Gnaq*RQ$^{fl/wt}$;E2a-Cre+ animals, we observed significantly increased pigmentation on the leptomeninges between the cerebellum and cortex, and between the cortex and the olfactory bulb (Figure 3B). Although low in numbers, melanocytes are present in the leptomeninges of the brain (Gudjohnsen et al. 2015). These cells are vulnerable to *GNAQ* mutations which can potentially induce

abnormal proliferation (Urtatiz et al. 2020).Therefore, this phenotype of enhanced melanocytic pigmentation in these particular areas of the brain, observed in the brains of older *Gnaq*RQ$^{fl/wt}$;E2a-Cre+ mice, is consistent with altered GNAQ signaling.

Due to the decreased number of live-born animals of the *Gnaq*RQ$^{fl/wt}$;E2a-Cre+ genotype, we sought to determine if there were any embryonic phenotypes associated with the observed loss of these mice during development. Therefore, we dissected embryos at e13.5-14.5 for gross morphological evaluation and genotyping. At this stage of development, we found normal, Mendelian ratios for all the expected genotypes (differences not significant by Chi-square test) (Figure 4A). However, in *Gnaq*RQ$^{fl/wt}$;E2a-Cre+ embryos, we observed prominent edema and some dilated small vessels in 50% (5 out of 10) and 20% (2 of 10) of the animals, respectively (Figure 4B). These findings indicate that mosaic expression of the mutant allele results in a severe embryonic phenotype in a significant number of *Gnaq*RQ$^{fl/wt}$;E2a-Cre+ mice that can eventually result in premature death.

Additionally, we examined *Gnaq* transcript levels in the *Gnaq*RQ$^{fl/wt}$;E2a-Cre+ embryos and found that levels of mutant transcript ranged between 43% to 100% (n=3) while the *Gnaq*RQ$^{fl/wt}$ embryos had 0% mutant transcript detectable (n=3) (Figure 4C). This range of mutant allele expression is expected due to the mosaic expression of the E2a Cre. We have previously noted that the highest mutant transcript levels in live-born animals that we found are approximately 50%; it is probable, that although e14.5 embryos are present with mutant transcript levels greater than 50%, these embryos are not surviving to birth.

Global expression of p.R183Q GNAQ is incompatible with survival

Our findings in the *Gnaq*RQ$^{fl/wt}$;E2a-Cre+ mice suggest that mosaic expression of the *Gnaq* mutant allele (p.R183Q) during development causes different degrees of pathology, the extent of which are likely due to the tissue location and the expression level of the mutant allele. Therefore, as a formal test of Happle's hypothesis, we next investigated the effect of global p.R183Q expression to determine if early global embryonic expression of the p.R183Q GNAQ mutation is compatible with survival. For this experiment, we crossed our *Gnaq*RQ conditional mutant strain with a transgenic line expressing a global (ubiquitous) β-actin Cre driver where the recombination occurs in the entire soma as early as the blastocyst stage (Lewandoski, Meyers, and Martin 1997).

Genotyping of mice at P0 in the cross between the β-actin Cre driver and our *Gnaq* inducible construct showed that no live-born mice contained both the Cre driver and the *Gnaq* conditional allele (Table 1) indicating that the p.R183Q GNAQ mutation causes embryonic lethality when globally expressed during the earliest stages of development.

To determine if and when the embryos expressing the mutant allele were present and if they displayed any phenotype, we examined mouse embryos at different stages of development. In initial observations of e11.5 and e14.5 embryos from crosses that would only yield β-actin-Cre positive embryos, we saw equal numbers of *Gnaq*RQ$^{wt/wt}$; Cre+ and *Gnaq*RQ$^{fl/wt}$;Cre+ embryos (data not shown). At e11.5, none of the *Gnaq*RQ$^{fl/wt}$;Cre+ embryos appeared different than littermate controls, but at e14.5,

*Gnaq*RQ$^{fl/wt}$;Cre+ embryos did show an overt vascular phenotype. Therefore, we decided to undertake a more systematic study with crosses designed to yield all four possible genotypes and to examine the embryos at e14.5. Genotypic analysis of larger numbers of embryos at e14.5 showed that the distribution of the four possible genotypes from the *Gnaq*RQ$^{wt/wt}$;β-actin-Cre+ x GnaqRQ$^{fl/wt}$ cross was normal (Table 1). We did note that of the resorbing embryos seen at e14.5 that we were able to genotype, a large percentage (72.7%, 8/11) were *Gnaq*RQ$^{fl/wt}$;β-actin-Cre+.

Using the SNaPshot transcript assay, we showed that the mutant *Gnaq* allele represented 100% of the total *Gnaq* transcript from *Gnaq*RQ$^{fl/wt}$;β-actin-Cre+ e14.5 embryos (Figure 5). These data demonstrate complete recombination of the targeted allele in *Gnaq*RQ$^{fl/wt}$;β-actin-Cre+ e14.5 embryos. These results from the e14.5 embryos, combined with the absence of any *Gnaq*RQ$^{fl/wt}$;β-actin-Cre+ pups born live, indicate that the *Gnaq*RQ$^{fl/wt}$;β-actin-Cre+ embryos are resorbed at some point during the third week of embryonic development. These results strongly suggest that global expression of p.R183Q GNAQ early during development is not compatible with survival, further supporting Happle's paradominant inheritance hypothesis.

Embryonic death in GnaqRQ$^{fl/wt}$;β-actin-Cre+ animals is associated with hemorrhage and vasodilation

Gross examination of *Gnaq*RQ$^{fl/wt}$;β-actin-Cre+ embryos demonstrated a variable phenotype. Although a small fraction of the *Gnaq*RQ$^{fl/wt}$;β-actin-Cre+ embryos appeared similar to their control littermates, a much higher percentage of *Gnaq*RQ$^{fl/wt}$;β-actin-Cre+ embryos demonstrated subcutaneous hemorrhage, edema, or were pale in

color compared to controls (Figure 6B). Genotype blinded examination of e14.5 embryos of all 4 possible genotypes showed hemorrhage in 86% of the *Gnaq*RQ$^{fl/wt}$;β-actin-Cre+ animals, which was often associated with subcutaneous edema (71%) (Table 2). By contrast, control littermates of all other genotypes did not exhibit any strong pathologies (Figure 6A). Mild hemorrhage and edema was reported only in one *Gnaq*RQ$^{wt/wt}$ embryo and in one *Gnaq*RQ$^{wt/wt}$;β-actin-Cre+ embryo, confirming that the severe phenotypes observed in *Gnaq*RQ$^{fl/wt}$;β-actin-Cre+ mice were associated with the expression of the mutant R183Q allele during development.

As most of these e14.5 embryos exhibited vascular abnormalities during gross examination, we performed histological assessment. Sagittal sections of the whole embryo revealed areas of extravasation in the subcutaneous region in *Gnaq*RQ$^{fl/wt}$;β-actin-Cre+ embryos, indicating severe alteration of blood vessel formation and circulation (Figure 6D, F, and J). Moreover, PECAM-1 immunostaining confirmed the presence of dilated blood vessels filled with red blood cells at sites of apparent hemorrhage in *Gnaq*RQ$^{fl/wt}$;β-actin-Cre+ embryos (Figure 6H and L), and was not seen in controls (Figure 6G and K). Instead, the blood vessels in *Gnaq*RQ$^{fl/wt}$ littermate controls were small, with only a few red blood cells visible in each vessel (Figure 6C, E, and I).

Downstream signaling effects

Constitutive activation of GNAQ caused by the p.R183Q somatic *GNAQ* mutation alters signaling pathways and distinct transcriptional programs implicated in vasculature development, angiogenesis, and blood vessel morphogenesis including angiopoietin-2

expression (Galeffi et al. 2022). A recent study reported that ANGPT2 expression was significantly increased both in human endothelial cultured cells expressing the R183Q mutation and in capillary malformations of SWS patients (Huang et al. 2022). Therefore, we performed qRT-PCR to measure *Angpt2* expression in e14.5 *Gnaq*RQ$^{fl/wt}$;β-actin-Cre+ embryos. We found that the level of *Angpt2* transcript was significantly higher in *Gnaq*RQ$^{fl/wt}$;β-actin-Cre+ embryos as compared to their *Gnaq*RQ$^{fl/wt}$ littermate controls (Figure 7).

Discussion

In our efforts to create a mouse model of SWS, we found that global mosaic expression of p.R183Q GNAQ with the "mosaic" E2a-Cre driver mouse line resulted in high levels of embryonic lethality. Among the postnatally viable *Gnaq*RQ$^{fl/wt}$;E2a-Cre+ animals, the levels of mutant *Gnaq* transcript expression were variable, reproducing the variable, mosaic recombination reported for this Cre line. The highest level of mutant transcript recorded among the postnatally viable *Gnaq*RQ$^{fl/wt}$;E2a-Cre+ animals was approximately 50%, suggesting that levels greater than 50% of mutant *Gnaq* transcript expression lead to prenatal lethality. This is further supported by the high levels of mutant transcript detected in *Gnaq*RQ$^{fl/wt}$;E2a-Cre+ embryos, strengthening the idea that high levels of p.R183Q GNAQ expression contribute to the embryonic lethality observed. We then found that ubiquitous global expression of p.R183Q GNAQ with the β-actin-Cre driver mouse line resulted in complete embryonic lethality in *Gnaq*RQ$^{fl/wt}$;β-actin-Cre+ animals and variable, but disease-relevant vascular phenotypes, in developing embryos. Vascular abnormalities in the embryos included grossly dilated

vessels and hemorrhage. The combined data using the two Cre drivers support Happle's hypothesis that this mutation would be lethal if passed through the germline.

The Genome Aggregation Database (gnomAD) of human DNA sequence variation in various populations provides further support of germline p.R183Q GNAQ lethality, albeit in the form of indirect evidence. As of January 5, 2023, the p.R183Q GNAQ mutation has not been reported in gnomAD, which includes sequence information from over 100,000 unrelated individuals. The embryonic lethality of the mutation is consistent with the known biochemical consequences of the mutation. The p.R183Q mutation in GNAQ has been shown to activate the G protein Gαq leading to increased downstream signaling (Shirley et al. 2013; Galeffi et al. 2022). Thus, this mutation might be postulated to be highly detrimental if globally expressed during development. The combined data from the human population, the biochemical consequences of the mutation, and the mouse model data presented here, all support Happle's 'paradominant inheritance' hypothesis – that this is a "lethal mutation surviving because of mosaicism".

Similar to the p.R183Q GNAQ mutation, mutations of glutamine 209 (Q209) result in activation of the GNAQ protein. While the p.R183Q GNAQ mutation results in a slowing of the GTP hydrolysis rate, p.Q209 GNAQ mutations result in irreversible, constitutive activation of the subunit (Kimple et al. 2011). Interestingly, the p.Q209 GNAQ mutation occurs frequently in uveal melanoma, a cancer of melanocytes in the uvea, the middle layer of the eye (Van Raamsdonk et al. 2010; Van Raamsdonk et al. 2009). In our model, we observed increased pigmentation of the leptomeninges in *Gnaq*RQ$^{fl/wt}$;E2a-

Cre+ adults, presumably in the melanocytes that are normally present in that location, further suggesting that our mouse model produces functional mutant protein. We note that the orthologous human p.R183Q GNAQ somatic mutation is also often found in uveal melanoma, (Van Trigt, Kelly, and Hughes 2022; Tate et al. 2019). We surmise then, that melanocytes are particularly sensitive to this mutation. Although the murine leptomeningeal melanocyte phenotype is not a SWS-associated phenotype that has been reported in patients, it is not clear whether this phenotype has ever been explored.

To date, two other animal models have been reported that examine mutant *GNAQ* in endothelial cells. In one approach, Matrigel plugs containing human endothelial cells expressing either WT or p.R183Q GNAQ were introduced into nude mice (Huang et al. 2022). This approach resulted in enlarged vascular lumens that resembled capillary malformations. In another approach, Matrigel plugs containing mouse Ms1 endothelial cells expressing p.Q209L GNAQ, a more strongly activating mutation, were introduced into nude mice (Sasaki et al. 2022). Through this approach, vascular tumors were identified and characterized. Although both models are useful in characterizing the role of GNAQ mutations in endothelial cells in the formation of vascular lesions, neither of these models are able to characterize the role and consequences of the p.R183Q GNAQ mutation during embryonic development. Other published models of mutant GNAQ endothelial cells rely on CMV promoters to drive expression of GNAQ, resulting in over-expression of this transcript relative to endogenous levels. Therefore, we targeted our conditional construct to the endogenous *Gnaq* locus. Moreover, to distinguish the conditional allele transcripts from those arising from the endogenous

allele, we inserted the poly(A) element from the BGH gene into the conditional allele. Despite our effort at maintaining physiological regulation of gene expression, allele specific qRT-PCR analysis revealed a significant increase in the levels of the conditional allele transcripts in both *Gnaq*RQ$^{fl/wt}$ and *Gnaq*RQ$^{fl/wt}$;Cre+ embryos, compared to the endogenous allele (Figure S2). Previous studies indicated that introduction of different poly(A) regions can have a significant effect on gene expression (Pfarr et al. 1986; Wang et al. 2022). Moreover, the introduction of the BGH poly(A) region results in a higher increase of recombinant mRNA expression (Pfarr et al. 1986; Wang et al. 2022) compared to other poly(A) elements tested due to efficient RNA stabilization (Pfarr et al. 1986). Despite the over-expression of both the wild-type and mutant transcripts from the conditional allele, we do not believe that overexpression *per se* (ie. overexpression of the wild-type allele) causes the vascular malformation phenotypes that we have observed. Even with a 2-fold increase in transcript expression from the conditional wild-type allele, *Gnaq*RQ$^{fl/wt}$ mice were born at the expected ratio and were phenotypically normal. We only observed embryonic lethality and severe vascular phenotypes in *Gnaq*RQ$^{fl/wt}$;Cre+ mice, strongly suggesting that only the expression of mutant transcript is correlated with the formation of the severe phenotype.

Here we have described the first mouse model with inducible expression of p.R183Q GNAQ, the causative mutation for SWS. We have also provided the first *in vivo* experimental evidence supporting the lethality of germline p.R183Q GNAQ. Intriguingly, deletion of both copies of murine *GNAQ* does not cause embryonic lethality, resulting in viable mice with relatively minor defects (impaired platelet activation and motor

coordination) (Offermanns, Toombs, et al. 1997) (Offermanns, Hashimoto, et al. 1997). Viability is likely due to compensation by the highly homologous and widely expressed GNA11 gene/protein (Offermanns et al. 1998). Thus, the normal function of *GNAQ* is not essential for development. By contrast, per Happle's paradominant inheritance hypothesis, inheritance of even a single copy of an *activated* (gain-of-function) *GNAQ* mutation leads to embryonic lethality, and thus, the p.R183Q mutation is only ever seen in a mosaic state. This inducible mouse model could be crucial in understanding the pathophysiology of SWS. Further studies using this conditional allele will be required to identify the developmental timeframe and the precise precursor cell(s) that must express the mutant transcript to fully recapitulate the SWS human phenotype.

Data availability

Mouse strains are available upon request.

Acknowledgements

The authors would like to acknowledge the Duke Transgenic Mouse Facility for generating the *Gnaq*RQ mouse model. We thank Drs. Christopher Counter and Özgün Le Roux for the kind gift of the ACTB$^{FLPe/FLPe}$ mice. This work was supported by the following grants: US Dept of Defense Medical Research Program Discovery Award W81XWH2110061 to DAM; 2020 Sturge-Weber Foundation Catalyst Award, and postdoctoral trainee position on T32 HL007101-45 to SEWS.

Conflicts of interest

None declared.

Table 1. Viable mice at e14.5 and P0 from *Gnaq*RQ$^{wt/wt}$;β-actin-Cre+ x *Gnaq*RQ$^{fl/wt}$ cross

Number of mice/ genotype					
Age	Total number	*Gnaq*RQ$^{wt/wt}$	*Gnaq*RQ$^{wt/wt}$; β-actin-Cre+	*Gnaq*RQ$^{fl/wt}$	*Gnaq*RQ$^{fl/wt}$; β-actin-Cre+
e14.5	70	15	22	19	14
P0	77	24	28	25	0

Table 2. Phenotypes observed at e14.5 from *Gnaq*RQ$^{wt/wt}$;β-actin-Cre+ x *Gnaq*RQ$^{fl/wt}$ cross

Genotype (e14.5)	Total number of embryos	Embryos with vascular anomaly	Embryos with edema
*Gnaq*RQ$^{wt/wt}$	15	1 (7%)	0
*Gnaq*RQ$^{wt/wt}$;β-actin-Cre+	22	0	1 (4%)
*Gnaq*RQ$^{fl/wt}$	19	0	0
*Gnaq*RQ$^{fl/wt}$;β-actin-Cre+	14	12 (86%)	10 (71%)

Figure 1. Demonstrating conditional p.R183Q GNAQ expression. A) The engineered construct was integrated into the endogenous *Gnaq* exon 4 as described in Figure S1. Cre-mediated recombination deletes the WT genomic sequence from the construct resulting in expression of the mutant *Gnaq*. B) To measure genomic recombination of the construct, primers 1 and 2 (black triangles) were designed to amplify the DNA

surrounding codon 183 from both the WT and the mutant R183Q sections of the engineered construct. The endogenous *Gnaq* locus cannot amplify under the conditions used since Primers 1 and 2 are located in separate exons; Primer 1 in exon 4 is separated from Primer 2 in exon 5 by almost 3 kb. SNaPshot analysis (a single base extension assay) at the site of the mutation shows equal amounts of both WT (G, blue peak) and mutant (A, green peak) in DNA from Cre- animals. In contrast, SNaPshot analysis from Cre+ animals shows that after Cre recombination, the WT section of the construct has been removed from the majority of cells leaving the mutant portion of the construct intact. C) Primers 3 and 4 (red triangles) were designed to measure the levels of WT and mutant transcription from the engineered construct. Primer 4 is located in the 3-UTR poly(A) site unique to the construct ensuring amplification from transcripts arising only from the engineered allele, not from the endogenous *Gnaq* allele. SNaPshot analysis of cDNA from Cre- animals shows that nearly all of the transcription comes from the WT portion of the construct while Cre+ animals show almost exclusive expression from the mutant portion of the construct.

Figure 2. Postnatal characterization of global but mosaic *Gnaq* expression. *Gnaq*RQ$^{fl/wt}$ animals were crossed to homozygous E2a-Cre+/+ animals and the resulting offspring were genotyped postnatally. The number of animals genotyped is shown on the bars for each category. *** $p<0.001$, by Chi-square test.

Figure 3. Postnatal phenotypes of *Gnaq*RQ;E2a-Cre mice. A) The mutant allele frequency from liver tissue cDNA was assessed by SNaPshot. The age range of the

animals was P21 to P391. B) Representative images of brains from postnatal animals with the leptomeninges intact. The brains from P21 animals are labeled and the other brains shown are from animals ranging in age from 4 – 6 months. Arrows indicate regions of increased pigmentation in *Gnaq*RQ$^{fl/wt}$;E2a-Cre+ animals.

Figure 4. Characterization of embryonic *Gnaq*RQ x E2a-Cre mice.

A) *Gnaq*RQ$^{fl/wt}$ animals were crossed to heterozygous E2a-Cre+ animals and the resulting offspring were dissected and genotyped at e13.5. The bars show the percentage of embryos present at e13.5 for each genotype. The number of animals genotyped is shown on the bars for each category. B) Representative images of embryos dissected at e13.5. The upper panel images of each timepoint show the embryo within the yolk sac with the placenta attached. Lower panel images show the same embryo removed from the yolk sac. White arrows point to areas of possible vascular malformations. Asterisks indicate edema. C) The mutant allele frequency from cDNA from whole e14.5 embryonic tissue was assessed by SNaPshot.

Figure 5. Mutant transcript analysis of e14.5 *Gnaq*RQ$^{fl/wt}$ and *Gnaq*RQ$^{fl/wt}$;β-actin-Cre+ embryos.

SNaPshot analysis was employed to assay the mutant allele transcript levels from whole embryo tissue. All of the *Gnaq*RQ$^{fl/wt}$ embryos had less than 5% mutant allele expression. Conversely, the *Gnaq*RQ$^{fl/wt}$;β-actin-Cre+ embryos all had mutant allele expression levels of 100%.

Figure 6. *Gnaq*RQ$^{fl/wt}$;β-actin-Cre+ embryos have hemorrhagic lesions and dilated vessels.

A) *Gnaq*RQ$^{fl/wt}$ embryo (control) at e14.5 exhibits normal morphology. B) *Gnaq*RQ$^{fl/wt}$;β-actin-Cre+ embryo exhibits extensive hemorrhage, dilated capillaries (as indicated by arrows) and subcutaneous edema (asterisk). C and D) Micrographs of parasagittal sections of e14.5 embryos stained with Hematoxylin and Eosin (H&E). The embryo of the *Gnaq*RQ$^{fl/wt}$;β-actin-Cre+ mouse shows extravasation and dilated vessels in different areas of the body including subcutaneous regions and in the leptomeninges. E and F) Higher power images (20 X) of the lower back region of the embryo (as indicated by the lower box in panels C and D) of control and *Gnaq*RQ$^{fl/wt}$;β-actin-Cre+ embryos. The arrow in F indicates dilated vessels, the asterisk indicates extravasation. G and H) PECAM-1 immunostaining, depicted in brown, confirmed the presence of dilated and abnormal vessels (arrow) in e14.5 embryos expressing the mutant *Gnaq*RQ allele compared to control. I, J, K, and L) Higher power images (20 X) of the leptomeningeal region (as indicated by the upper box in panels C and D) demonstrate severe vascular alterations in the *Gnaq*RQ$^{fl/wt}$;β-actin-Cre+ embryo compared to control (arrows). Bar in panel C represents 1 mm (scale for C and D). Bar in panel E represents 100 μm (scale for panels E-L).

Figure 7. Downstream signaling effect of mutant *Gnaq* expression.

qRT-PCR results showing *Angpt2* expression in tissue from e14.5 embryos. Expression of *Angpt2* is significantly increased in embryos expressing mutant *Gnaq*. All embryos examined contained one copy of the conditional allele. Data represent the mean ± SEM,

n=5 and 3 for *Gnaq*RQ$^{fl/wt}$ and *Gnaq*RQ$^{fl/wt}$;β-actin-Cre+, respectively. *p=0.035 unpaired two-tailed Student's *t*-test.

References

Galeffi, F., D. A. Snellings, S. E. Wetzel-Strong, N. Kastelic, J. Bullock, C. J. Gallione, P. E. North, and D. A. Marchuk. A novel somatic mutation in GNAQ in a capillary malformation provides insight into molecular pathogenesis. Angiogenesis. 2022.

Gudjohnsen, S. A., D. A. Atacho, F. Gesbert, G. Raposo, I. Hurbain, L. Larue, E. Steingrimsson, and P. H. Petersen. Meningeal Melanocytes in the Mouse: Distribution and Dependence on Mitf. Front Neuroanat. 2015; 9: 149.

Happle, R. Lethal genes surviving by mosaicism: a possible explanation for sporadic birth defects involving the skin. J. Am. Acad. Dermatol. 1987; 16: 899-906.

Huang, L., C. Bichsel, A. L. Norris, J. Thorpe, J. Pevsner, S. Alexandrescu, A. Pinto, D. Zurakowski, R. J. Kleiman, M. Sahin, A. K. Greene, and J. Bischoff. Endothelial GNAQ p.R183Q Increases ANGPT2 (Angiopoietin-2) and Drives Formation of Enlarged Blood Vessels. Arterioscler Thromb Vasc Biol. 2022; 42: e27-e43.

Keum, S., H. K. Lee, P. L. Chu, M. J. Kan, M. N. Huang, C. J. Gallione, M. D. Gunn, D. C. Lo, and D. A. Marchuk. Natural genetic variation of integrin alpha L (Itgal) modulates ischemic brain injury in stroke. PLoS Genet. 2013; 9: e1003807.

Kimple, A. J., D. E. Bosch, P. M. Giguere, and D. P. Siderovski. Regulators of G-protein signaling and their Galpha substrates: promises and challenges in their use as drug discovery targets. Pharmacol. Rev. 2011; 63: 728-49.

Lakso, M., J. G. Pichel, J. R. Gorman, B. Sauer, Y. Okamoto, E. Lee, F. W. Alt, and H. Westphal. Efficient in vivo manipulation of mouse genomic sequences at the zygote stage. Proc Natl Acad Sci U S A. 1996; 93: 5860-5.

Lee, H. K., D. H. Kwon, D. L. Aylor, and D. A. Marchuk. A cross-species approach using an in vivo evaluation platform in mice demonstrates that sequence variation in human RABEP2 modulates ischemic stroke outcomes. Am J Hum Genet. 2022; 109: 1814-27.

Lewandoski, M., E. N. Meyers, and G. R. Martin. Analysis of Fgf8 gene function in vertebrate development. Cold Spring Harb. Symp. Quant. Biol. 1997; 62: 159-68.

Offermanns, S., K. Hashimoto, M. Watanabe, W. Sun, H. Kurihara, R. F. Thompson, Y. Inoue, M. Kano, and M. I. Simon. Impaired motor coordination and persistent multiple climbing fiber innervation of cerebellar Purkinje cells in mice lacking Galphaq. Proc Natl Acad Sci U S A. 1997; 94: 14089-94.

Offermanns, S., C. F. Toombs, Y. H. Hu, and M. I. Simon. Defective platelet activation in G alpha(q)-deficient mice. Nature. 1997; 389: 183-6.

Offermanns, S., L. P. Zhao, A. Gohla, I. Sarosi, M. I. Simon, and T. M. Wilkie. Embryonic cardiomyocyte hypoplasia and craniofacial defects in G alpha q/G alpha 11-mutant mice. EMBO J. 1998; 17: 4304-12.

Pfarr, D. S., L. A. Rieser, R. P. Woychik, F. M. Rottman, M. Rosenberg, and M. E. Reff. Differential effects of polyadenylation regions on gene expression in mammalian cells. DNA. 1986; 5: 115-22.

Rodriguez, C. I., F. Buchholz, J. Galloway, R. Sequerra, J. Kasper, R. Ayala, A. F. Stewart, and S. M. Dymecki. High-efficiency deleter mice show that FLPe is an alternative to Cre-loxP. Nat Genet. 2000; 25: 139-40.

Sasaki, M., Y. Jung, P. North, J. Elsey, K. Choate, M. A. Toussaint, C. Huang, R. Radi, A. J. Perricone, V. G. Corces, and J. L. Arbiser. Introduction of Mutant GNAQ into Endothelial Cells Induces a Vascular Malformation Phenotype with Therapeutic Response to Imatinib. Cancers (Basel). 2022; 14.

Shirley, M. D., H. Tang, C. J. Gallione, J. D. Baugher, L. P. Frelin, B. Cohen, P. E. North, D. A. Marchuk, A. M. Comi, and J. Pevsner. Sturge-Weber syndrome and port-wine stains caused by somatic mutation in GNAQ. N Engl J Med. 2013; 368: 1971-9.

Tate, J. G., S. Bamford, H. C. Jubb, Z. Sondka, D. M. Beare, N. Bindal, H. Boutselakis, C. G. Cole, C. Creatore, E. Dawson, P. Fish, B. Harsha, C. Hathaway, S. C. Jupe, C. Y. Kok, K. Noble, L. Ponting, C. C. Ramshaw, C. E. Rye, H. E. Speedy, R. Stefancsik, S. L. Thompson, S. Wang, S. Ward, P. J. Campbell, and S. A. Forbes. COSMIC: the Catalogue Of Somatic Mutations In Cancer. Nucleic Acids Res. 2019; 47: D941-D47.

Uchiyama, Y., M. Nakashima, S. Watanabe, M. Miyajima, M. Taguri, S. Miyatake, N. Miyake, H. Saitsu, H. Mishima, A. Kinoshita, H. Arai, K. Yoshiura, and N. Matsumoto. Ultra-sensitive droplet digital PCR for detecting a low-prevalence somatic GNAQ mutation in Sturge-Weber syndrome. Scientific reports. 2016; 6: 22985.

Urtatiz, O., C. Cook, J. L. Huang, I. Yeh, and C. D. Van Raamsdonk. GNAQ(Q209L) expression initiated in multipotent neural crest cells drives aggressive melanoma of the central nervous system. Pigment Cell Melanoma Res. 2020; 33: 96-111.

Van Raamsdonk, C. D., V. Bezrookove, G. Green, J. Bauer, L. Gaugler, J. M. O'Brien, E. M. Simpson, G. S. Barsh, and B. C. Bastian. Frequent somatic mutations of GNAQ in uveal melanoma and blue naevi. Nature. 2009; 457: 599-602.

Van Raamsdonk, C. D., K. G. Griewank, M. B. Crosby, M. C. Garrido, S. Vemula, T. Wiesner, A. C. Obenauf, W. Wackernagel, G. Green, N. Bouvier, M. M. Sozen, G. Baimukanova, R. Roy, A. Heguy, I. Dolgalev, R. Khanin, K. Busam, M. R. Speicher, J. O'Brien, and B. C. Bastian. Mutations in GNA11 in uveal melanoma. N Engl J Med. 2010; 363: 2191-9.

Van Trigt, W. K., K. M. Kelly, and C. C. W. Hughes. GNAQ mutations drive port wine birthmark-associated Sturge-Weber syndrome: A review of pathobiology, therapies, and current models. Front Hum Neurosci. 2022; 16: 1006027.

Ventura, A., D. G. Kirsch, M. E. McLaughlin, D. A. Tuveson, J. Grimm, L. Lintault, J. Newman, E. E. Reczek, R. Weissleder, and T. Jacks. Restoration of p53 function leads to tumour regression in vivo. Nature. 2007; 445: 661-5.

Wang, X. Y., Q. J. Du, W. L. Zhang, D. H. Xu, X. Zhang, Y. L. Jia, and T. Y. Wang. Enhanced Transgene Expression by Optimization of Poly A in Transfected CHO Cells. Front Bioeng Biotechnol. 2022; 10: 722722.

Figure 1

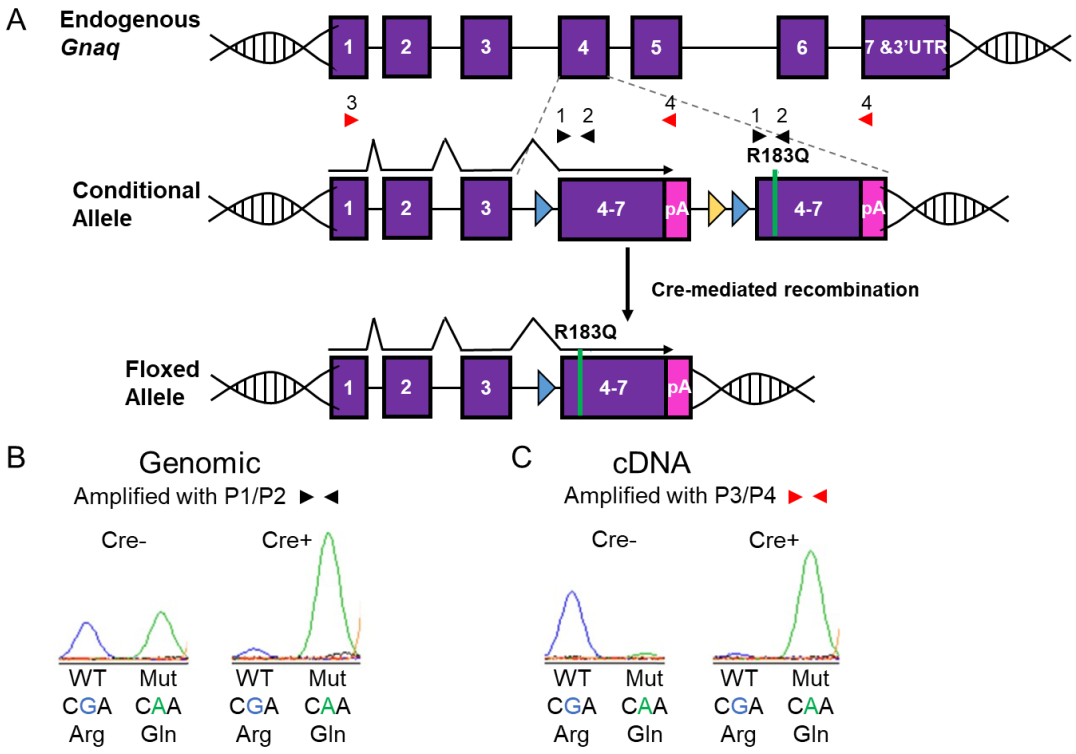

Figure 2

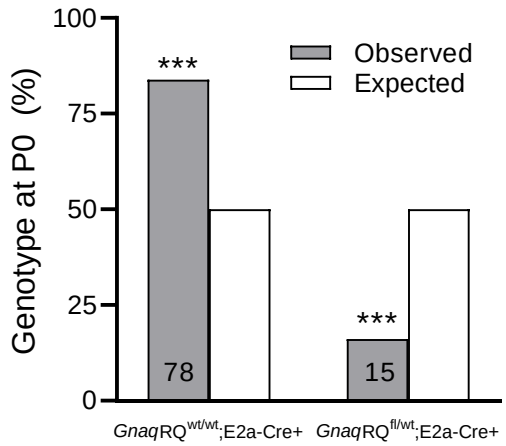

Figure 3

A

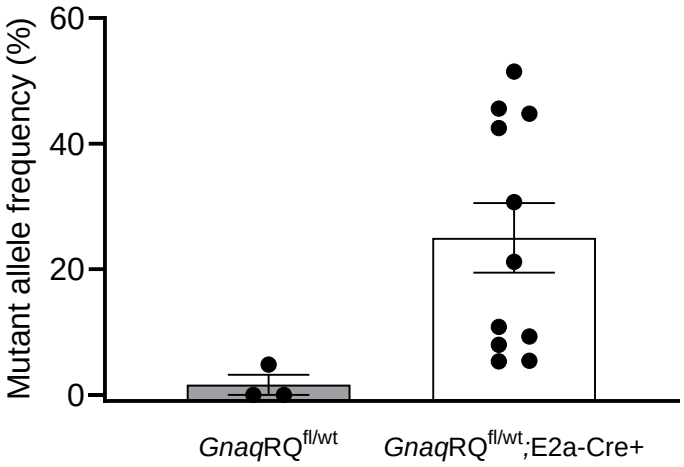
Mutant allele frequency (%)
60
40
20
0
GnaqRQfl/wt
GnaqRQfl/wt;E2a-Cre+

B

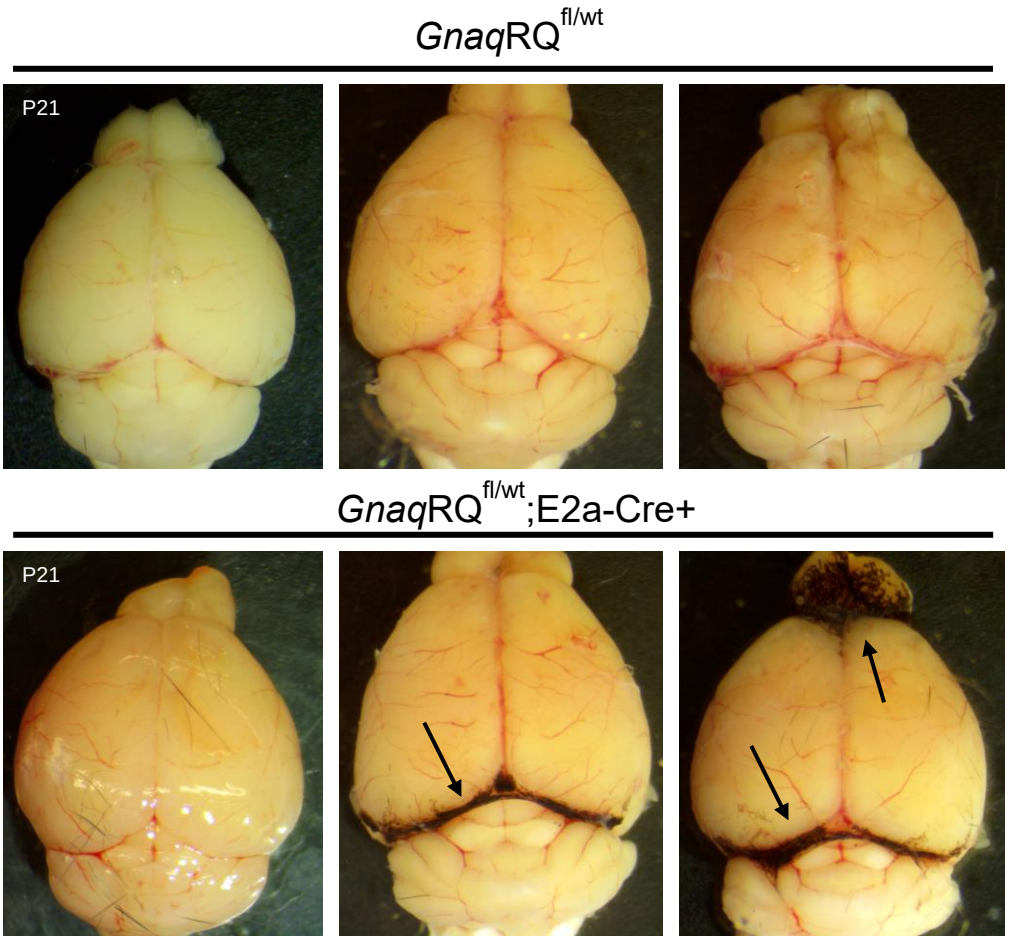
GnaqRQfl/wt
P21
GnaqRQfl/wt;E2a-Cre+
P21

Figure 4

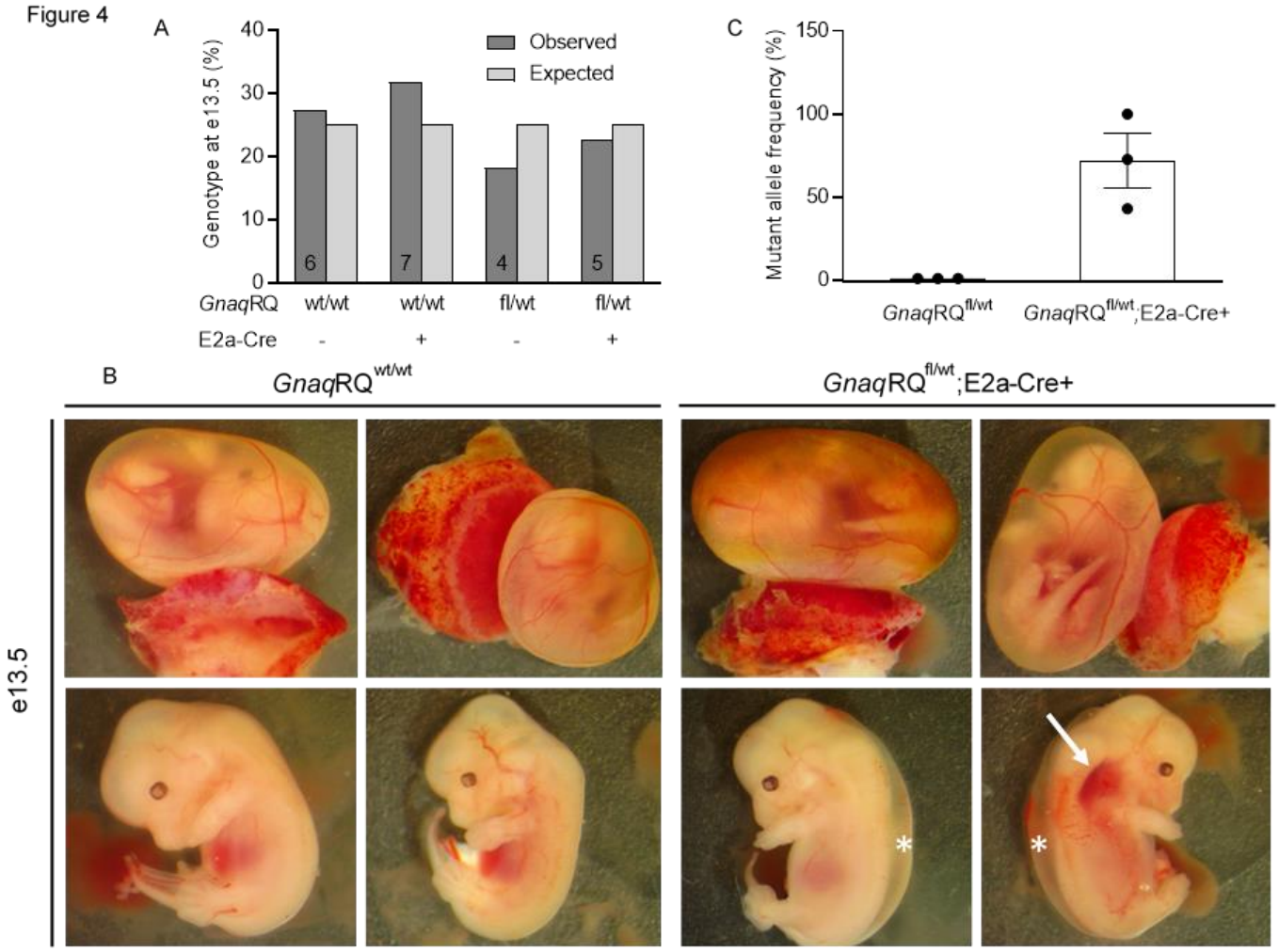

Figure 5

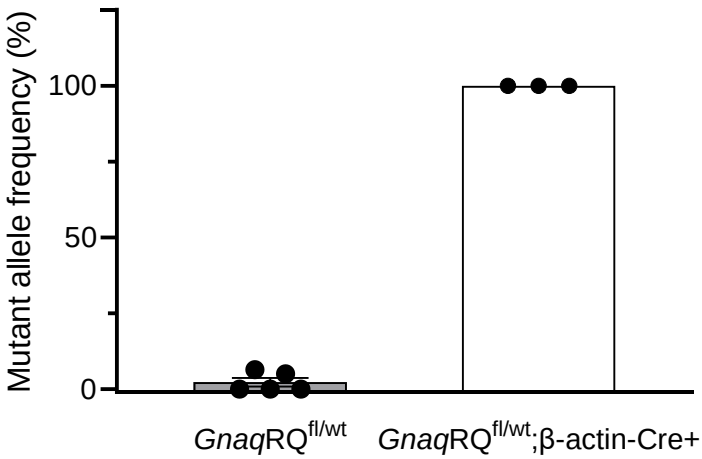

Figure 6

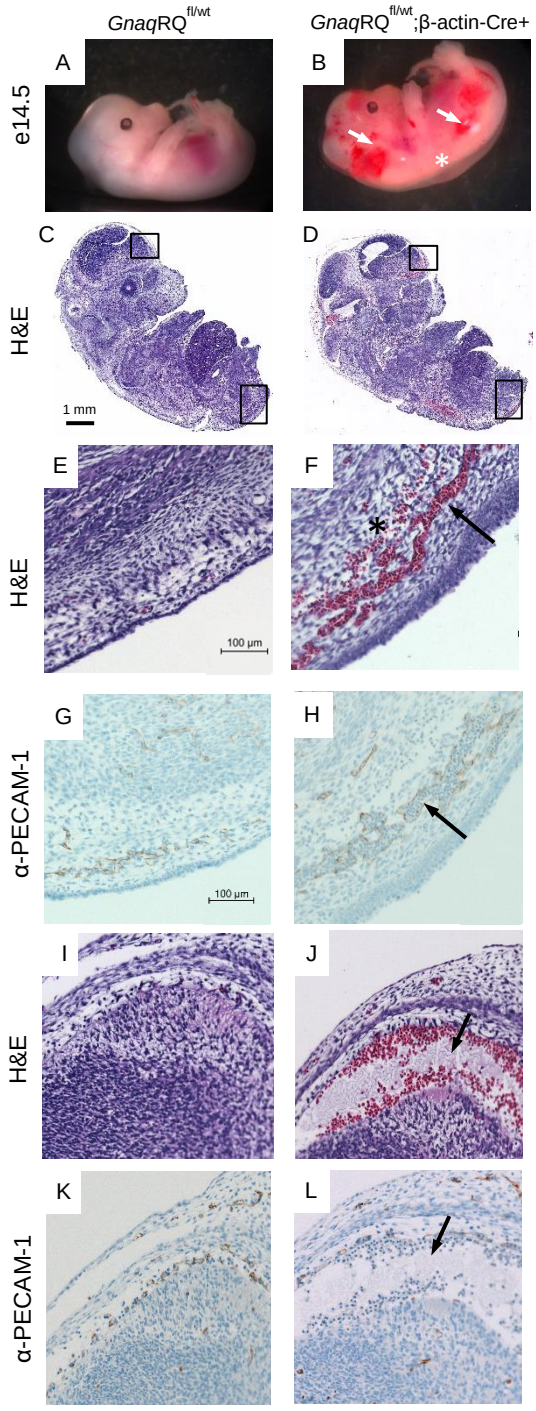
GnaqRQfl/wt
GnaqRQfl/wt;β-actin-Cre+
A
B
e14.5
C
D
H&E
1 mm
E
F
H&E
100 µm
G
H
α-PECAM-1
100 µm
I
J
H&E
K
L
α-PECAM-1

Figure 7

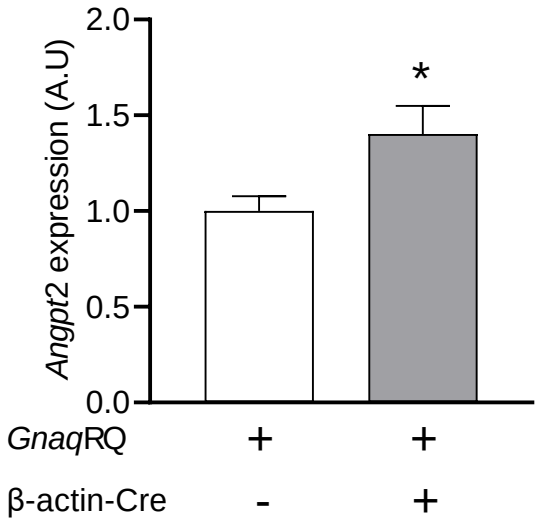

Figure S1

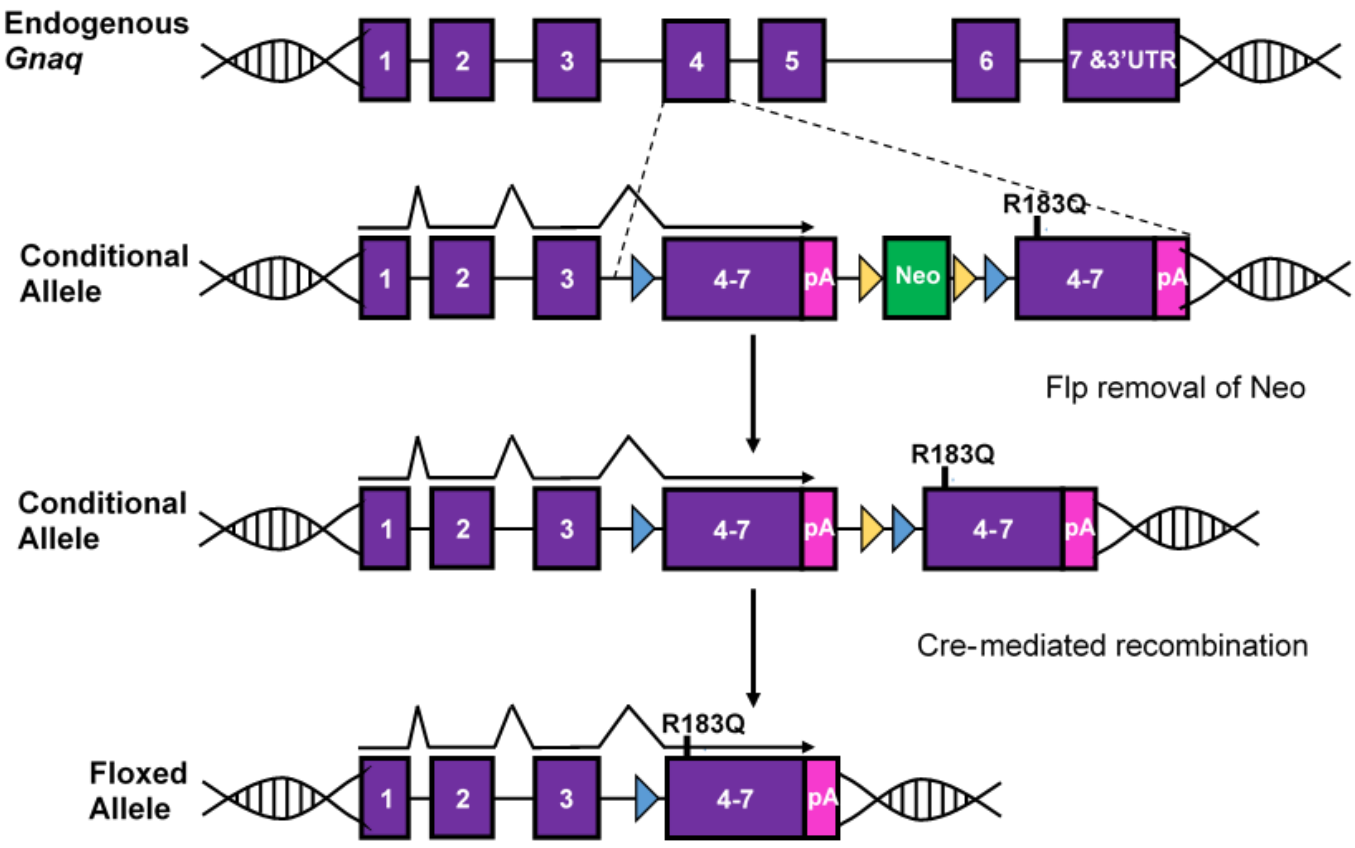

Figure S1. *Gnaq*RQ Mouse Gene Targeting Approach

Homologous recombination was used to replace the endogenous exon 4 of *Gnaq* with a construct allowing for Cre recombinase-dependent expression of p.R183Q GNAQ. The following elements were present in the targeting construct: 1) a cDNA block of mouse *Gnaq* exons 4-7 encoding the WT form of the protein, 2) a neomycin resistance cassette (green box) flanked by FRT sites (yellow triangles) for FRT-mediated recombination, 3) loxP sites (blue triangles) for Cre mediated recombination of the WT *Gnaq* cDNA block and the FRT site, and 4) a cDNA block of mouse *Gnaq* exons 4-7 encoding the p.R183Q mutant form of the protein. The 3'UTR and poly(A) site from Bovine growth hormone 1 (BGH1, pink block denoted pA) was ligated to the 3' end of exon 7 to provide a way to distinguish transcripts from the conditional allele from the endogenous *Gnaq*.

Figure S2

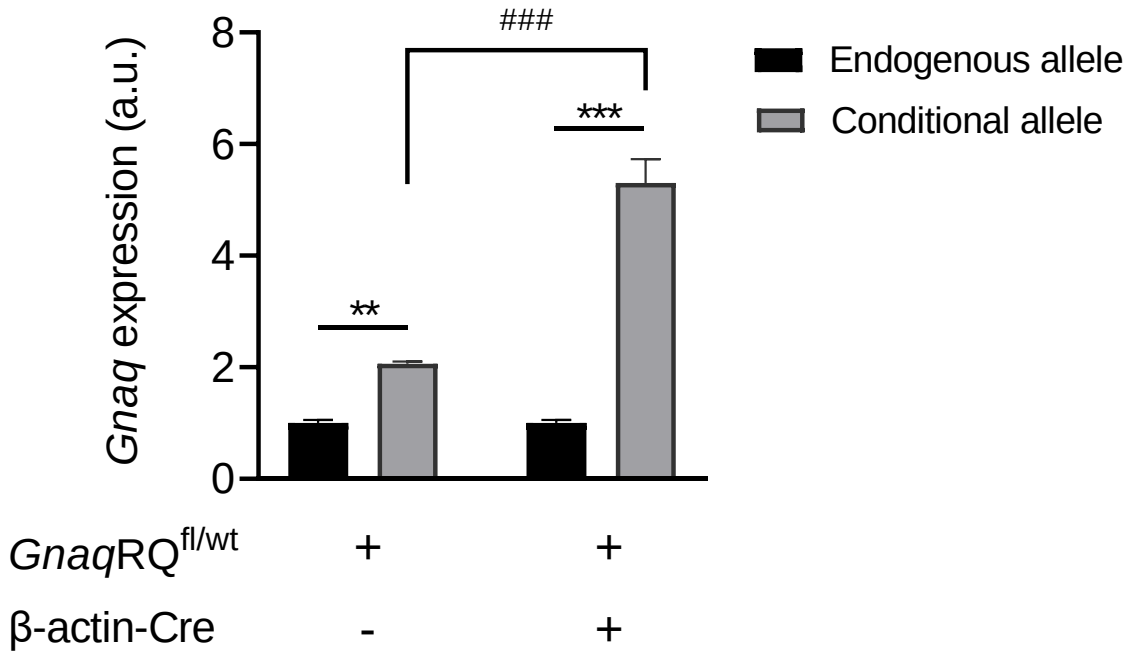

Figure S2. *Gnaq* transcript levels in embryos from *Gnaq*RQ$^{fl/wt}$ x *Gnaq*RQ$^{fl/wt}$;β-actin-Cre+ cross. qRT-PCR results from e14.5 embryonic mouse tissue from *Gnaq*RQ$^{fl/wt}$ and *Gnaq*RQ$^{fl/wt}$;β-actin-Cre+ littermates using allele specific primers revealed that *Gnaq* conditional allele transcripts were significantly higher than transcripts from the endogenous allele in both groups ($p^{***} = 0.0002$ and $p^{**} = 0.007$ conditional *vs* endogenous allele, for *Gnaq*RQ$^{fl/wt}$ and *Gnaq*RQ$^{fl/wt}$;β-actin-Cre+, respectively, two tailed paired *t*-test) with a greater increase in *Gnaq*RQ$^{fl/wt}$;β-actin-Cre+ ($p^{###} < 0.001$ *Gnaq*RQ$^{fl/wt}$;β-actin-Cre+ vs *Gnaq*RQ$^{fl/wt}$, two tailed unpaired *t*-test).